



저작자표시-비영리-변경금지 2.0 대한민국

이용자는 아래의 조건을 따르는 경우에 한하여 자유롭게

- 이 저작물을 복제, 배포, 전송, 전시, 공연 및 방송할 수 있습니다.

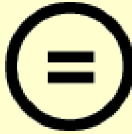
다음과 같은 조건을 따라야 합니다:



저작자표시. 귀하는 원저작자를 표시하여야 합니다.



비영리. 귀하는 이 저작물을 영리 목적으로 이용할 수 없습니다.



변경금지. 귀하는 이 저작물을 개작, 변형 또는 가공할 수 없습니다.

- 귀하는, 이 저작물의 재이용이나 배포의 경우, 이 저작물에 적용된 이용허락조건을 명확하게 나타내어야 합니다.
- 저작권자로부터 별도의 허가를 받으면 이러한 조건들은 적용되지 않습니다.

저작권법에 따른 이용자의 권리는 위의 내용에 의하여 영향을 받지 않습니다.

이것은 [이용허락규약\(Legal Code\)](#)을 이해하기 쉽게 요약한 것입니다.

[Disclaimer](#)

In situ reprogramming by nano-hypoxia of  
spleen to instruct therapeutic homing of  
vasculogenic cells

Seyong Chung

Department of Medicine

The Graduate School, Yonsei University

# In situ reprogramming by nano-hypoxia of spleen to instruct therapeutic homing of vasculogenic cells

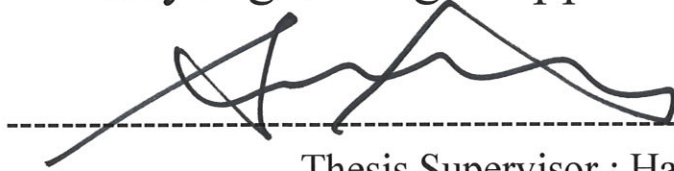
Directed by Professor Hak-Joon Sung

Doctoral Dissertation  
submitted to the Department of Medicine,  
the Graduate School of Yonsei University  
in partial fulfillment of the requirements for the degree of  
Doctor of Philosophy in Medical Science

Seyong Chung

December 2023

This certifies that the Doctoral Dissertation of  
Seyong Chung is approved.



Thesis Supervisor : Hak-Joon Sung



Thesis Committee Member#1 : Boyoung Joung



Thesis Committee Member#2 : Jong-Chul Park

Thesis Committee Member#3: Hee Tae Yu



Thesis Committee Member#4: Dae-Hyun Kim

The Graduate School  
Yonsei University

December 2023

## ACKNOWLEDGEMENTS

The Harvard Study of Adult Development, which followed 814 adults for over 70 years, identified 'high educational level' as one of the conditions for happiness. When I first heard this while attending medical school, I thought that 'high educational level' led to happiness because it led to better jobs, income, or status. Now, about 15 years later, with M.D. and Ph.D. added after my name, my thoughts have changed a bit. A high level of education can make a person happy in itself, separate from the benefits it brings, and I believe all education has its value. I do not regret the choices I have made over the past 15 years and am proud to encourage my two sons to achieve a high level of education.

I want to express my gratitude to my beloved wife Hye Jee Ryoo, who I want to spend the rest of my happy life with, and my two sons, who always manage to drain and recharge my energy. What I have achieved would not have been possible without the help of my respected father, mother, father-in-law, and mother-in-law. I would like to express my gratitude to Professor Hak-Joon Sung, who provided much inspiration and guidance during my Ph.D. program; Professor Boyoung Joung, who was my advisor during my master's program and will continue to guide me; and to Professor Jong-Chul Park, Hee Tae Yu, and Dae-Hyun Kim, for serving as members of my thesis defense committee. Lastly, I would like to express my gratitude to the senior, colleague, and junior members of my lab who were with me during my doctoral studies.

## <TABLE OF CONTENTS>

ABSTRACT .....	v
I. INTRODUCTION .....	1
1. Spleen-mediated targeting .....	1
2. Vasculogenic cell treatment .....	3
3. Nano-hypoxia as a key linker of the targeting and the treatment .....	5
4. Object of thesis .....	6
II. MATERIALS AND METHODS .....	8
1. Liposome preparation .....	8
2. Animal experiments .....	9
3. Splenic mononuclear cell culture .....	9
4. In vitro studies for facilitated angiogenesis effect of vasculogenic cells .....	10
5. Animal studies for liposomal targeting to spleen .....	11
6. Animal studies for in vivo reprogramming of splenic mononuclear cells .....	11
7. Animal studies using vascular disease model of hindlimb ischemia .....	13
8. Animal studies using tissue regeneration model of 70 % hepatectomy .....	14
9. Biosafety evaluation for nano-hypoxia .....	15
10. 3D chip model for evaluating vasculogenic cell homing ability .....	15
11. IF study .....	16
12. PCR .....	17
13. FACS .....	18
14. Statistical analysis .....	19
III. RESULTS .....	20
1. Nano-hypoxia for splenic in situ reprogramming towards vasculogenic cells .....	20
A. The effect of hypoxia during culture of splenic mononuclear cells .....	20

B. The effect of a hypoxic-mimetic agent on the culture .....	22
C. Nano-hypoxia as a vasculogenic reprogrammer of the cells .....	25
D. In situ reprogramming strategy by nano-hypoxia in mice .....	27
E. Validation of the reprogramming effect .....	30
F. Secured vasculogenic cell amounts in the strategy .....	32
2. Spleen-mediated targeting even after the reprogramming .....	34
A. 3D chip model .....	34
B. In vivo models .....	36
3. Therapeutic efficacy in preclinical models .....	40
A. Mouse hindlimb ischemia model .....	40
B. Biosafety of nano-hypoxia .....	44
C. Mouse 70 % hepatectomy model .....	47
IV. DISCUSSION .....	51
V. CONCLUSION .....	54
REFERENCES .....	55
ABSTRACT(IN KOREAN) .....	63
PUBLICATION LIST .....	65

## LIST OF FIGURES

Figure 1. Splenic capture of nanoparticles doesn't have to be a hurdle for targeting .....	1
Figure 2. In situ reprogramming strategy is simple, non-invasive, and effective .....	3
Figure 3. Roles of hypoxia and hypoxic-mimetic agent (cobalt) .....	6
Figure 4. Hypoxia reprogrammed splenic mononuclear cells towards vasculogenic cells .....	21
Figure 5. Reprogrammed vasculogenic cells facilitate angiogenesis ..	23
Figure 6. Nano-hypoxia delivers hypoxic reprogramming effect in vitro .....	26
Figure 7. Nano-hypoxia delivers hypoxic reprogramming effect in vivo .....	28
Figure 8. Validation of hypoxic reprogramming effect of nano-hypoxia .....	31
Figure 9. Advantage in vasculogenic cell amounts of in situ reprogramming .....	33
Figure 10. Targeting of vasculogenic cells in 3D chip model .....	35
Figure 11. Targeting of vasculogenic cells in in vivo models .....	38
Figure 12. In situ reprogramming in mouse hindlimb ischemia model .....	42

Figure 13. Biosafety of nano-hypoxia .....	45
Figure 14. In situ reprogramming in mouse 70 % hepatectomy model .....	49

## LIST OF TABLES

Table 1. Primers .....	18
------------------------	----

## ABSTRACT

**In situ reprogramming by nano-hypoxia of spleen to instruct therapeutic homing of vasculogenic cells**

Seyong Chung

*Department of Medicine  
The Graduate School, Yonsei University*

(Directed by Professor Hak-Joon Sung)

Splenic capture of the targeting nanoparticles is one of the major reasons for only 0.7 % of the injected dose, on average from meta-analysis, being located in the target sites. However, the spleen doesn't need to be a hurdle if those captured nanoparticles move to the target sites with splenocytes since splenic mononuclear cells inherently target the inflammatory sites. One possible application for this is vasculogenic cell treatment, which has shown unmet needs in terms of dose and delivery limitations in clinical trials. Here, splenic mononuclear cells were in situ reprogrammed by nano-hypoxia towards vasculogenic cells. Hypoxic-mimetic agent-loaded nanoparticles were captured by splenic mononuclear cells, and the resulting cells were validated for facilitating angiogenesis. Also, secured vasculogenic cells are at >20-fold the conventional dose, and they inherently target inflammatory sites in an inflammatory degree-dependent manner, effectively addressing the dose and delivery issues. Consequently, the in situ reprogramming strategy demonstrated superiority over the conventional strategy regarding angiogenesis facilitation and the recovery of blood flow in a mouse hindlimb ischemia model. This strategy was also effective in enhancing angiogenesis and subsequent liver regeneration in a mouse 70 % hepatectomy model. In conclusion, the in situ reprogramming strategy using nano-hypoxia of the spleen can address the unmet needs of dose and delivery limitations in current vasculogenic cell treatment.

---

Key words : targeting nanoparticle, spleen, inflammatory sites, vasculogenic cell, angiogenesis

## In situ reprogramming by nano-hypoxia of spleen to instruct therapeutic homing of vasculogenic cells

Seyong Chung

*Department of Medicine  
The Graduate School, Yonsei University*

(Directed by Professor Hak-Joon Sung)

### I. INTRODUCTION

#### 1. Spleen-mediated targeting

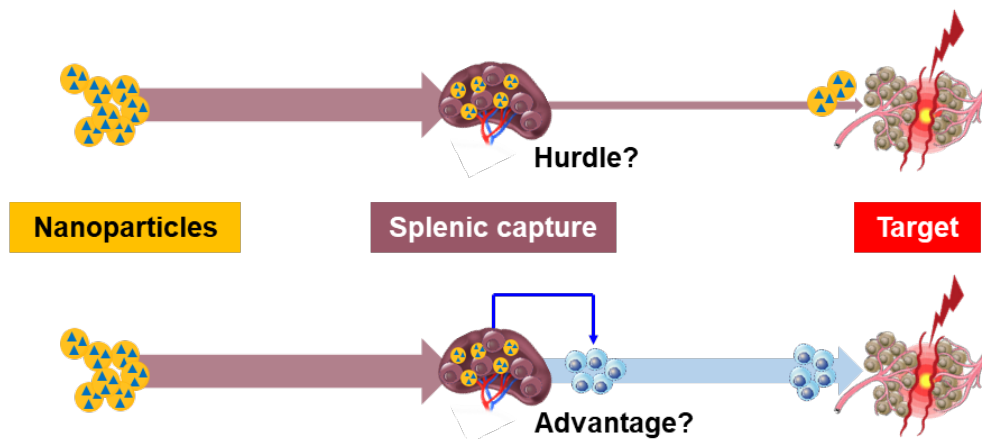


**Figure 1.** Splenic capture of nanoparticles doesn't have to be a hurdle for targeting<sup>1</sup>.

"Targeting" is one of the strongest advantages of using nanoparticles, and advanced targeting strategies can further improve their theranostic efficacy. However, a meta-analysis from a publication spanning 10 years revealed that, on average, only 0.7 % of the injected nanoparticles reach the target<sup>2</sup>. This number may still be higher than the targeting efficiency of conventional free drugs<sup>3-6</sup>, but it explains the limited clinical

application of nanoparticles<sup>2,7,8</sup>.

When nanoparticles are introduced into the systemic circulation with the goal of targeting specific locations, they may encounter and be captured by off-target sites before reaching the intended targets. The major cell populations that capture these nanoparticles are immune cells known as the mononuclear phagocyte system (MPS), which is typically distributed in the spleen and liver<sup>1-4,7-12</sup>.

This capture by the MPS doesn't have to be a hurdle for targeting only if they move to the target sites (**Figure 1**). Indeed, immune cells are inherently attracted to inflammatory sites as a means of the body's defense mechanism<sup>1,13-24</sup>. Additionally, the spleen is known as a reservoir of undifferentiated monocytes that can be deployed to inflammatory sites, such as myocardial ischemia and cerebral ischemia<sup>1,13-18,20,22,23</sup>.

Strategizing spleen-mediated targeting comes with numerous advantages. First, the targeting efficiency can be dramatically improved since the spleen captures a large portion of nanoparticles<sup>1-4,7-12</sup>. Even the small fraction of those spleen-captured nanoparticles that are supposed to move to the target sites could be a significant amount considering the current targeting efficiency of 0.7 %<sup>2</sup>.

Second, more accurate targeting, even without a targeting moiety, can be achieved since this spleen-mediated targeting relies on the inherent distribution of nanoparticles to the spleen and immune cells to the inflammatory sites. Targeting is commonly strategized by attaching a specific targeting moiety to the nanoparticles, such as proteins, peptides, nucleic acids, or small molecules<sup>3,5-8,12,25,26</sup>. This so-called 'active' targeting showed a slight improvement in targeting efficiency (0.9 %) <sup>2</sup>, but among the few clinically approved nanoparticles, those with a targeting moiety have not yet passed clinical trials<sup>7</sup>. This may be caused by additional hurdles in the manufacturing process provoked by attaching a targeting moiety to the nanoparticles<sup>7</sup>. The absence of the need for those targeting moieties is surely an advantage of this spleen-mediated targeting.

Third, the immune cells that carry nanoparticles to the target sites may raise new perspectives to maximize the theranostic efficiency. By priming those cells in sync with

theranostic intentions, this spleen-mediated targeting may exhibit the advantages of cell therapy beyond the simple drug delivery to the target sites.

## 2. Vasculogenic cell treatment

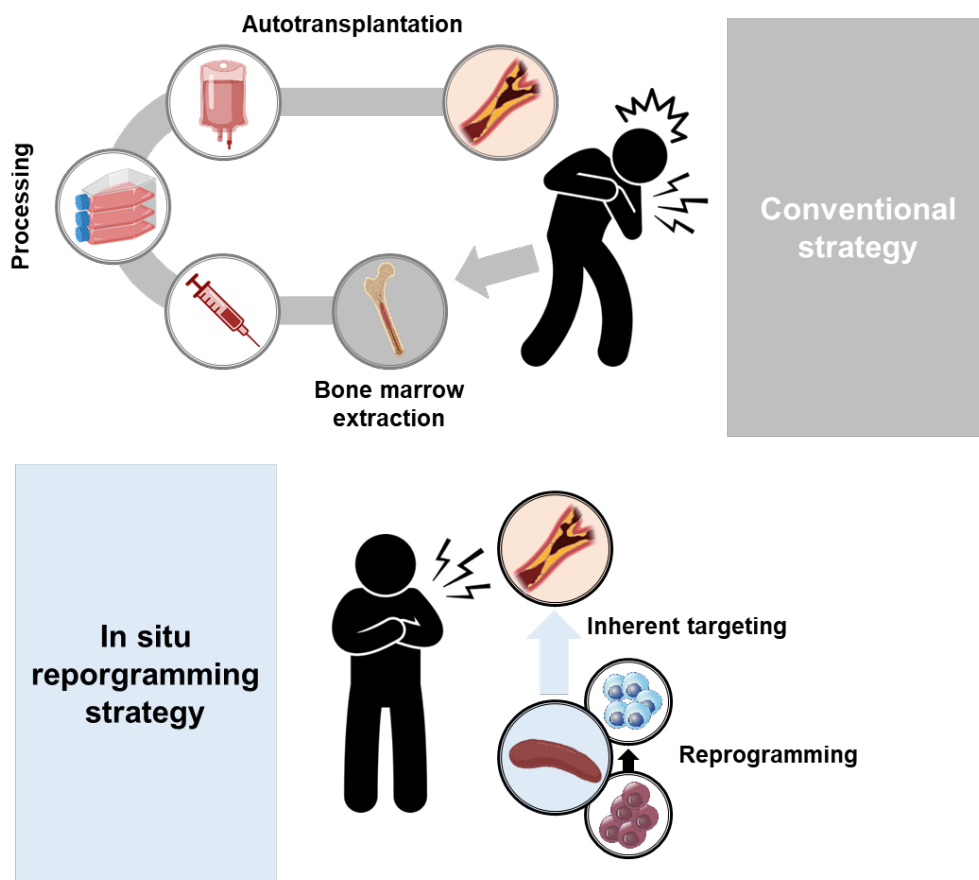


**Figure 2.** In situ reprogramming strategy is simple, non-invasive, and effective<sup>1</sup>.

Since mononuclear cells were first illuminated as potential "vasculogenic cells" in 1997<sup>27</sup>, implanting these cells at ischemic sites has been considered an original and potent modality to promote angiogenesis<sup>28-45</sup>. The usual approach starts with extracting

mononuclear cells from bone marrow<sup>28,29,31,32,34,35,38-45</sup> or blood<sup>27,30,33,36,41</sup>, which are then autotransplanted to the ischemic sites with or without some ex vivo processing procedures. In addition to ischemic sites, vasculogenic cell treatment has also been applied to many diseases, such as liver<sup>46-49</sup>, lung<sup>50</sup>, and neuron<sup>51,52</sup> damage. For example, angiogenesis is a key factor in the process of liver regeneration after hepatectomy<sup>46,47,49,53</sup>, and vasculogenic cell treatment has improved the regeneration<sup>46,49</sup>.

Numerous clinical trials were followed in patients with coronary artery disease<sup>54-60</sup> or peripheral artery disease<sup>61-64</sup>, but most of these trials have shown only marginal therapeutic effects, falling short of expectations<sup>65-70</sup>. One of the earliest randomized clinical trials was the BOOST trial in 2004, which demonstrated some therapeutic potential of vasculogenic cell treatment<sup>54</sup>. However, in the BOOST-2 trial of 2017, the same research group concluded that this treatment showed no improvement in cardiac function<sup>60</sup>. In fact, a meta-analysis of 41 randomized clinical trials involving 2732 patients revealed no therapeutic effect on all-cause mortality, cardiovascular mortality, or any other single or composite endpoint related to reinfarction, re-hospitalization, or quality of life<sup>70</sup>.

There are several points that need to be discussed in order to improve the therapeutic effect. First, an insufficient dose of vasculogenic cells could be one reason for the unsatisfactory results. Some review papers have commented on the need to refine the appropriate therapeutic dose<sup>65,66,68</sup>, and a clinical trial has demonstrated the dose-dependent effect of vasculogenic cell treatment<sup>57</sup>. However, since these vasculogenic cells are prepared from the patients' bone marrow or blood cells, dramatically increasing the yield is difficult in the conventional setting. Some studies have attempted ex vivo expansion of vasculogenic cells<sup>27,30,33,34,37</sup>, but effective culture methods are also demanding and not readily available<sup>65</sup>.

Another point to be addressed is the delivery of vasculogenic cells<sup>65,66,69</sup>. In most clinical studies, vasculogenic cells are autotransplanted at the site of ischemia<sup>54-64</sup>, and for patients with coronary artery disease, an additional transcatheter approach to the

coronary artery was performed, risking unnecessary bleeding or thrombosis<sup>54-60</sup>. Furthermore, the extraction process of bone marrow is also a painful and risky procedure, as shown in clinical trials that used sedation or anesthesia during the process and interrupted aspirin administration to avoid bleeding<sup>55,57,59</sup>. However, these problems are also difficult to completely eliminate as long as we stick to the conventional autotransplantation strategy of extracting and re-injecting cells.

What if all the processes of autotransplantation were performed inside the body? Mononuclear cells are generated in the bone marrow and stored abundantly in the spleen<sup>13-15,17</sup>. Furthermore, splenic mononuclear cells can also be used for vasculogenic cell treatment<sup>37</sup>. If only those stored cells could be primed *in vivo* and inherently target the ischemic sites, it could actually help resolve the issues mentioned above (**Figure 2**).

### 3. Nano-hypoxia as a key linker of the targeting and the treatment

So, how can we prepare vasculogenic cells in the spleen? To date, there are many agents that can be used for priming mononuclear cells<sup>71</sup>, and hypoxia is one of them<sup>1,71-74</sup>. Mononuclear cells can become vasculogenic simply by being exposed to hypoxia<sup>1,73</sup>, which increases the expression of vascular endothelial growth factor (VEGF)<sup>71-81</sup>. Besides, hypoxia are known to beneficial for maintaining vasculogenic cell characteristics<sup>72,77-87</sup> and promoting angiogenesis<sup>71,72,74-81,86-88</sup>.

Then, how can we put spleen under hypoxia? Most of the effects by hypoxia are through the hypoxia-inducible factor 1 $\alpha$  (HIF-1 $\alpha$ ) protein<sup>72-81,83,84,86,88-97</sup>. HIF-1 $\alpha$  protein is translated in most of the cells regardless of the oxygen concentration, but degraded by prolyl hydroxylase domain enzymes in the existence of oxygen and iron<sup>1,75,76,78,79,81,86,89-93,97</sup>. Thus, HIF-1 $\alpha$  expression is upregulated in hypoxic conditions.

In same reason, HIF-1 $\alpha$  expression can be upregulated in the absence of iron<sup>1,75,76,86,88-93,97</sup>. This is the basic principles of some hypoxic-mimetic agents which chelates or competes with iron (**Figure 3**). For example, cobalt has similar atomic number (27) with

iron (26), so it can competitively inhibits iron and widely used as a hypoxic-mimetic agents<sup>1,72,75,76,86,88-97</sup>. Similarly, targeting spleen with cobalt-loaded nanoparticles may serves as a way to put spleen under hypoxia, which also can be called “nano-hypoxia”. If this nano-hypoxia could turn splenic mononuclear cells to vasculogenic cells, it can link spleen-mediated targeting to vasculogenic cell treatment.

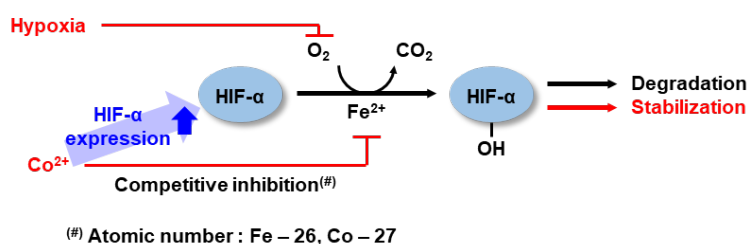


**Figure 3.** Roles of hypoxia and hypoxic-mimetic agent (cobalt)<sup>1</sup>.

#### 4. Object of thesis

The purpose of this study is establishing an original treatment strategy on ischemic sites based on instructing spleen-derived vasculogenic cells. By applying spleen-mediated targeting to the vasculogenic cell treatment, this ‘in situ reprogramming’ strategy could include most aforementioned advantages and may lead to better outcomes than conventional treatment strategies.

First, the effect of nano-hypoxia on splenic mononuclear cells should be evaluated. This evaluation will be conducted in both in vitro and in vivo settings, and the difference between hypoxia and nano-hypoxia should also be evaluated.

Second, the spleen-mediated targeting should be validated for applying to the vasculogenic cell treatment. Especially, whether the targeting ability remains after hypoxic reprogramming in splenic mononuclear cells should be checked.

Lastly, the therapeutic efficacy of our strategy will be confirmed in comparison with

conventional strategy of vasculogenic cell treatment. Also, the biosafety of our strategy should be evaluated.

## II. MATERIALS AND METHODS

### 1. Liposome preparation

Liposomes was prepared by rapid injection method (for liposome with cargo). 1,2-dipalmitoyl-sn-glycero-3-phosphocholine (DPPC; 850355P, Sigma-Aldrich, St. Louis, MO, USA), cholesterol (C8667, Sigma-Aldrich), 1,2-distearoyl-sn-glycero-3-phosphoethanolamine-N-[methoxy(polyethylene glycol)-2000] (DSPE-PEG; 880120P, Sigma-Aldrich) were dissolved (55:40:5 molar ratio) in ethanol (E7023, Sigma-Aldrich) at 72 °C to be the final concentration of 200 mmol/L. Using 20-gauge needle (Koreavaccine, Seoul, Republic of Korea) and syringe (Restek, Bellefonte, PA, USA), this lipid mixture was rapidly injected to the same volume of cargo-containing solution under vigorous stirring of 500 rotations per minutes (RPM) at 72 °C; for cargo-containing solution, CoCl<sub>2</sub> (C8661, Sigma-Aldrich) solution (1 M) was used for CoCl<sub>2</sub>-loaded liposomes, and 5 nm gold nanoparticle solution (752568, Sigma-Aldrich) was used for gold nanoparticle-encapsulated liposomes. After 5 minutes, quadruple volume of cargo-containing solution (same solution in previous step) was added and kept stirring for 15 minutes in room temperature. Additionally, to tag <sup>19</sup>F on CoCl<sub>2</sub>-loaded liposomes, ethanol was substituted by 19:1 (v/v) solution of ethanol and 1H,2H,2H,2H-perfluorohexan-1-ol (532770, Sigma-Aldrich).

After manufacturing liposomes, liposome size was adjusted by extruding 100 nm-sized polycarbonate membrane filter (PCT019030, Sterlitech, Auburn, WA, USA) for 12 times, using Avanti mini-extruder (610000, Sigma-Aldrich) and filter support (610014, Sigma-Aldrich). Then, liposomes were gathered by centrifugation at 30,000 g for 1 hour in 4 °C, and resuspended to phosphate-buffered saline (PBS; LB004, Welgene, Gyeongsan, Republic of Korea; for in vitro use) or 0.9 % normal saline (NS; for in vivo use; JW Pharmaceutical, Seoul, Republic of Korea). Unloaded cargoes were removed by tubing dialysis (molecular weight cut off 12-14 kDa; 132706, Repligen, Waltham, MA, USA)

overnight before centrifugation.

Additionally, fluorescence-tagged liposomes were prepared by labelling DiD (V22887, Thermo Fisher, Waltham, MA, USA) to liposomes according to the manufacturer's instruction.

The morphology and size of liposomes were examined by transmission electron microscopy (TEM; Jem2100, JEOL, Tokyo, Japan) and nanoparticle tracking analysis (NS300, Malvern Panalytical, Malvern, UK). To check cargo ( $\text{CoCl}_2$ ,  $^{19}\text{F}$ ) encapsulation and concentration in liposomes, inductively coupled plasma (ICP; Nexion 2000, Perkin Elmer) was used for  $\text{CoCl}_2$ , and nuclear magnetic resonance (Avance III HD 400, Bruker, Billerica, MA, USA) was used for  $^{19}\text{F}$  (dissolved in  $\text{D}_2\text{O}$ ).

## 2. Animal experiments

The Yonsei University College of Medicine's Institutional Animal Care and Use Committee granted approval for all animal studies (Permit No. 2022-0050). C57BL/6 (male, 6 weeks old; Orient Bio, Gyeonggido, Republic of Korea) were used. For administration of liposome, liposome was injected into tail vein after anesthetized with intraperitoneal injection of zoletil (50 mg/kg; Virbac, Seoul, Republic of Korea) and xylazine (10 mg/kg; Bayer, Leverkusen, Germany). In mice experiments with fluorescence-tagged liposome, diet without auto-fluorescence (D10001, Central Lab. Animal Inc., Seoul, Republic of Korea) were fed for more than one week before experiments. For sacrifice,  $\text{CO}_2$  gas was used.

## 3. Splenic mononuclear cell culture

Spleen was harvested from sacrificed mouse, and splenic mononuclear cells were isolated using CD11b selection kit (480110, Biolegend, San Diego, CA, USA). Cells were seeded in culture plate ( $3 \times 10^6$  cells/ $\text{cm}^2$ ) and cultured with RPMI 1640 medium

(11875-093, Thermo Fisher) supplemented with fetal bovine serum (FBS; 10 % w/v; 16000-044, Thermo Fisher) and penicillin-streptomycin (PS; 1 % w/v; 15140-122, Thermo Fisher) in incubator (5 % CO<sub>2</sub>, 37 °C).

For hypoxic priming, cells were incubated in hypoxia incubator (1 % O<sub>2</sub>; 4131, Thermo Fisher), or cultured with CoCl<sub>2</sub> (100 μM) for 72 hours, with changing medium daily. CoCl<sub>2</sub> was added in form of CoCl<sub>2</sub> solution (15862, Sigma-Aldrich) or CoCl<sub>2</sub>-loaded liposomes. After priming, cells were used for optical imaging (Dmi8, Leica Microsystems, Wetzlar, Germany), immunofluorescence (IF) study and polymerase chain reaction (PCR); for IF study, DAPI (H1200, Vectashield, Darmstadt, Germany), anti-CD11b (1:200; ab8878, Abcam, Waltham, MA, USA), anti-CD34 (1:200; ab81289, Abcam), anti-stem cell antigen 1 (SCA1) (1:200; ab51317, Abcam), anti-HIF-1α (1:50; NB100-105, Novus, Centennial, CO, USA), secondary anti-rat Alexa Flour 594 (1:500; 712-585-150, Jackson Lab, Bar Harbor, ME, USA), secondary anti-rabbit Alexa Flour 488 (1:500; 111-545-003, Jackson Lab), and secondary anti-mouse Alexa Flour 680 (1:500; 715-625-150, Jackson Lab) were used (see the IF study or PCR section below for details).

#### 4. In vitro studies for facilitated angiogenesis effect of vasculogenic cells

To evaluate the facilitated angiogenic effect of vasculogenic cells, vasculogenic cells and human umbilical vein endothelial cells (HUVEC; passage 3-6; Lonza, Basel, Switzerland) were co-cultured in transwell with 0.4 μm pore (35024, SPL, Seoul, Republic of Korea). Splenic mononuclear cells or vasculogenic cells were prepared in transwell's upper chamber by using medium with or without CoCl<sub>2</sub> (see the splenic mononuclear cell culture section above for details). Then, in new transwell's lower chamber, 250 μL of matrigel (354234, Corning, Steuben County, NY, USA) was coated, followed by seeding 5 \* 10<sup>4</sup> HUVEC with endothelial cell growth medium 2 (EGM-2) supplemented with EGM-2 Bullet Kit (CC-3162, Lonza). At the same time, new

transwell's (empty) upper chamber was substituted by prepared transwell's upper chamber (with splenic mononuclear cells or vasculogenic cells). After 4 hours of co-culture in transwell, tubulogenesis was checked by optical imaging and analyzed by angiogenesis analyzer tool of Image J (National Institutes of Health, Bethesda, MD, USA).

Furthermore, supernatant from upper chamber with splenic mononuclear cells or vasculogenic cells were subjected for measurement of VEGF by enzyme-linked Immunosorbent assay kit (900-K10, Peprotech, Cranbury, NJ, USA).

Also, to evaluate the facilitated angiogenesis effect in inflammatory situations, LPS (L8274, Sigma-Aldrich) was treated (1  $\mu\text{g}/\text{mL}$ ) for HUVEC at 24 hours before seeding to transwell; so, HUVEC with or without LPS treatment were co-cultured with vasculogenic cells in transwell, and tubulogenesis was checked after 4 hours.

#### 5. Animal studies for liposomal targeting to spleen

To check splenic mononuclear cell targeting of  $\text{CoCl}_2$ -loaded liposomes, they were injected to tail vein, and mice were sacrificed at 72 hours after injection to harvest spleen. Cobalt amount in spleen and liver were evaluated by ICP.

For comparing splenic mononuclear cells to other splenocytes, liposomes were injected after tagged with DiD fluorescence. Mice were sacrificed at 72 hours after injection, and two cell groups of harvested spleen were separated by CD11b selection kit. Then, the fluorescence intensity of each cell groups were measured by in vivo imaging system (IVIS; 124262, Perkin Elmer).

Meanwhile, to check the location of cargo inside the spleen, gold nanoparticle-loaded liposomes were used instead of  $\text{CoCl}_2$ -loaded liposome, and spleen was harvested after sacrificed at 72 hours for TEM imaging.

#### 6. Animal studies for in vivo reprogramming of splenic mononuclear cells

For in vivo reprogramming by nano-hypoxia, CoCl<sub>2</sub>-loaded liposomes were injected (500 ng for cobalt amount). Mice were sacrificed at 72 hours from injection, and spleen was harvested for IF study and fluorescence-activated cell sorting (FACS); for IF study, DAPI, anti-CD11b (1:200), anti-CD34 (1:200), anti-SCA1 (1:200), secondary anti-rat Alexa Flour 594 (1:500), and secondary anti-rabbit Alexa Flour 488 (1:500) were used on frozen section; for FACS, anti-CD11b with FITC (3 µg/mL; MA1-10081, Thermo Fisher), anti-CD45 with allophycocyanin (APC) (2.5 µg/mL; 147708, Biolegend), anti-CD34 with phycoerythrin(PE)-cyanine 7 (5 µg/mL; 119326, Biolegend), anti-vascular endothelial (VE) cadherin with PE-cyanine 7 (10 µg/mL; 138016, Biolegend), and anti-c-Kit with APC-cyanine 7 (2.5 µg/mL; Biolegend, 135136) were used (see the IF study, or FACS section below for details).

To evaluate the impact of nano-hypoxia against conventional strategies involving bone marrow cells, bone marrow cells were extracted from femur. For extraction of bone marrow cells, mice were sacrificed and femur was carefully disassociated from muscles, ligaments, and tendons. After excising the lower end of femur to expose marrow cavity, femur was put into 0.5 mL centrifuge tube (PCR-05-C, Corning), prepared in advance for drill a hole at bottom with 20-gauge needle. This tube was inserted to larger (1.7 mL) centrifuge tube (MCT-175-C, Corning), and spun at 10,000 g for 15 seconds. The marrow that flows out through bottom hole of 0.5 mL tube to 1.7 mL tube was subjected for FACS (same as nano-hypoxia above). Also, the number of cell was counted in both cells from splenic nano-hypoxia and cells from bone marrow using automated cell counter (Countess II, Thermo Fisher).

For in vivo reprogramming by splenic artery ligation, mice were anesthetized by zoletil (50 mg/kg) and xylazine (10 mg/kg), and spleen was exposed to microscopy lens by abdominal incision. Splenic artery was identified and ligated 2 times using 9-0 ethilon (2829G, Ethicon, Raritan, NJ, USA), followed by closing abdomen using 4-0 black silk (SK434, Ailee, Busan, Republic of Korea). Mice were sacrificed at 72 hours from

ligation and spleen was harvested for FACS (same as nano-hypoxia above).

#### 7. Animal studies using vascular disease model of hindlimb ischemia

For hindlimb ischemia, mice were anesthetized by zoletil (50 mg/kg) and xylazine (10 mg/kg), and skin was shaved and incised to expose left femoral artery and vein. Then, upper and lower points of femoral artery and vein were ligated using 6-0 black silk (SK517, Ailee), followed by closing skin using 4-0 black silk. Meanwhile, in hindlimb ischemia/reperfusion group, upper point of femoral artery and vein were temporary ligated only for 1 hour and reperused, to induce paradoxical severe ischemic damage.

To evaluate the vasculogenic homing ability, ICP, IVIS, and magnetic resonance imaging (MRI) were used. For ICP,  $\text{CoCl}_2$ -loaded liposomes were injected at 72 hours before surgery, and mice were sacrificed at 24 hours from surgery. Spleen, liver and ischemic hindlimb were harvested and cobalt amount of each organ was measured by ICP. For IVIS, fluorescence-tagged  $\text{CoCl}_2$ -loaded liposomes were injected at 72 hours before surgery, and mice were sacrificed at 24 hours from surgery. Spleen was harvested and subjected for IVIS imaging. For MRI,  $^{19}\text{F}$ -tagged  $\text{CoCl}_2$ -loaded liposomes were injected at 72 hours before surgery, and MRI (9.4T BioSpec, Bruker) was conducted at 24 hours from surgery under anesthetized by isoflurane (Ifran, Hana Pharm, Seongnam, Republic of Korea) inhalation. Using  $^1\text{H}/^{19}\text{F}$  transceive surface coil, T2-weighted  $^1\text{H}$  images were acquired using fast spin echo protocol for reference image, and then the coil was tuned to  $^{19}\text{F}$  frequency for spectroscopic imaging experiments using the following MRI parameters; field of view 40 x 40 mm, free induction decay mode, repetition time 1,000 ms, spin echo 50,000 Hz, and 1,800 scans with 41 averages. Spectra were acquired for the voxel size of 8 x 8, and then processed to 16 x 16. Data were further analyzed using MATLAB (MathWorks, Natick, MA, USA).

To evaluate the therapeutic effect of nano-hypoxia,  $\text{CoCl}_2$ -loaded liposomes were injected into tail vein at 72 hours before surgery in nano-hypoxia group, while bone

marrow cells ( $10^7$  cells in 100  $\mu$ L of NS) were directly injected into ischemic site before closing the skin. For laser doppler imaging of blood flow (0, 7 and 14 days after surgery), LDPI (Moor Instruments, Devon, UK) was used under anesthetized by zoletil (50 mg/kg) and xylazine (10 mg/kg). For MRI imaging of blood flow (14 days after surgery), mice were anesthetized by isoflurane inhalation, and 200  $\mu$ L of MRI contrast (Clariscan, GE Healthcare, Chicago, IL, USA) was injected into tail vein. T1-weighted images were obtained using the following MRI parameters; field of view 50 x 50 x 15 mm, matrix size 256 x 150 x 20, repetition time 13.820 ms; echo time 1.818 ms, flip angle 19.8 degrees, signal average 1, scan time 5 minutes and 13 seconds. Mice were euthanized 14 days after surgery, and the tissue from the ischemic hindlimb was prepared for hematoxylin and eosin (H&E) staining, IF study, and PCR; for IF study, DAPI, anti-CD31 (1:100; NB600-562, Novus), anti-von Willebrand factor (vWF) (1:1000; NB600-586), secondary anti-mouse Alexa Flour 594 (1:500), and secondary anti-rabbit Alexa Flour 488 (1:500) were used on paraffin section (see the IF study section below for details).

#### 8. Animal studies using tissue regeneration model of 70 % hepatectomy

For partial hepatectomy, mice were anesthetized by zoletil (50 mg/kg) and xylazine (10 mg/kg), and skin was shaved and incised to expose liver. Using bipolar vessel sealing instruments (LigaSure Technology, Medtronic, Dublin, Ireland), left lateral lobe and median lobe were serially resected. To check the splenic dependence of nano-hypoxia effect, spleen was optionally removed in some mice using bipolar vessel sealing instruments. Peritoneum and skin were serially closed using 4-0 black silk. In nano-hypoxia group, CoCl<sub>2</sub>-loaded liposomes were injected at 72 hours before surgery. Mice were sacrificed either at 48 or 96 hours after surgery, since the proliferation of hepatocytes is peaked before 48 hours, while the resulted regeneration of liver was evaluated at 96 hours<sup>98</sup>.

To check the liver size change, computed tomography (CT; Quantum GX2, Perkin Elmer) scanning was conducted at before, immediately after, and 96 hours after surgery using 200  $\mu$ L of CT contrast (Iodixanol, GE Healthcare). Regeneration of liver was also measured by harvested liver weight per body weight after sacrifice. To check the liver function, blood concentration of bilirubin was measured at 96 hours after surgery. To check angiogenesis and hepatocyte proliferation of liver, H&E staining and IF study was done; for IF study, DAPI, anti-CD31 (1:100), anti-vWF (1:1000), anti- VEGF (1:200; ab2349, Abcam), anti-Ki-67 (1:200; ab16667, Abcam), secondary anti-mouse Alexa Flour 594 (1:500), and secondary anti-rabbit Alexa Flour 488 (1:500) were used on paraffin section (see the IF study section below for details).

#### 9. Biosafety evaluation for nano-hypoxia

To evaluate hepatotoxicity of  $\text{CoCl}_2$ -loaded liposomes, blood concentration of aspartate aminotransferase, alanine aminotranferase, alkaline phosphatase and bilirubin were measured using automated clinical chemistry analyzer (DRI-CHEM NX500i, Fuji Film, Tokyo, Japan).

To evaluate hematotoxicity of  $\text{CoCl}_2$ -loaded liposomes, buffer solution (from CD11b selection kit) was used to prepare 3 different groups - no treat group, injection dose group (42  $\mu$ M of  $\text{CoCl}_2$ -loaded liposome), and positive control group (100 mM  $\text{CoCl}_2$  solution). Next, each of these solutions (20  $\mu$ L) were placed on separate slide glasses, and mouse blood (2  $\mu$ L) obtained by tail vein transection was added to each one. A cover glass was applied, and the resulting samples were optically imaged at 0, 4, and 24 h.

#### 10. 3D chip model for evaluating vasculogenic cell homing ability

To evaluate homing ability of vasculogenic cells to inflammatory tissues in 3D chip model, vasculogenic cells were prepared by reprogramming splenic mononuclear cells

with  $\text{CoCl}_2$  (see the splenic mononuclear cell culture section above for details), and tissues were gained from ischemic (tissue with inflammation) or contralateral (tissue without inflammation) hindlimb of hindlimb ischemia model (see the vascular disease model section above for details) using 1 mm biopsy punch (69031-01, Integra LifeScience, Princeton, NJ, USA). Cells and tissues were labelled by DiD and DiO (V22886, Thermo Fisher), respectively, according to the manufacturer's instruction.

For 3D chip model, hydrogel chip with microchannel network was prepared from our previous study, using PNIPAM (535311, Sigma-Aldrich) as sacrificing structural materials. Using custom-made spinning device (2,500-2,800 RPM) with PNIPAM in methanol (53 % w/v; 106009, Merck Millipore, Burlington, MA, USA), microvasculature-mimetic fiber (average diameter of 16  $\mu\text{m}$ ) was obtained. In custom-made mold of 7 (width) x 7 (depth) x 5 (height) mm size, 11.45  $\mu\text{g}/\text{mm}^3$  of fibers were embedded, followed by pouring 9:1 mixture of gelatin (5.5 % w/v in PBS; G1890, Sigma-Aldrich) and microbial transglutaminase (mTG; 10 % w/v in PBS; 1201-50, Modernist Pantry, Eliot, ME, USA). Then, tissues (with or without inflammation) were inserted at both ends of the chip, and vasculogenic cells were injected at halfway point of tissues. Chip was incubated at 37 °C for 30 minutes for gelatin-mTG crosslinking, followed by pouring PBS (room temperature) to sacrifice PNIPAM fibers. 26-gauge needle was stucked at center top of the chip and connected to syringe pump for media perfusion; 20  $\mu\text{L}/\text{minute}$  for RPMI 1640 medium supplemented with FBS (10 % w/v) and PS (1 % w/v). Viability of tissues and homing of vasculogenic cells were evaluated after 24 hours of incubation (5 %  $\text{CO}_2$ , 37 °C), using live & dead assay kit (L3224, Thermo Fisher) and confocal microscopy (LSM 980, Carl-Zeiss, Oberkochen, Germany).

## 11. IF study

In this study, IF study was conducted using in vitro samples, in vivo samples with paraffin section or frozen section. For in vitro samples, samples were cultured in 24 well

plate with glass bottom (P24-1.5P, Cellvis, Mountain View, CA, USA), followed by fixed with 4 % paraformaldehyde (PFA; CNP015-0500, CellNest, Hanam, Republic of Korea) and permeabilized with 0.2 % Triton X-100 (93443, Sigma-Aldrich). Then, the samples were treated with 5 % bovine serum albumin (BSA; 82-100-6, Merck Millipore) to block them, and followed by treating antibodies. For in vivo samples with paraffin section, sample were fixed in 10 % neutral buffered formalin (F2013, Biosesang, Seongnam, Republic of Korea) solution for 24 hours followed by embedding in paraffin. After making sections in 4  $\mu\text{m}$  thickness, samples were deparaffinized and rehydrated, and followed by treating antibodies. For in vivo samples with frozen section, samples were embedded in optimal cutting temperature compound (3801480, Leica Biosystems, Nussloch, Germany) and frozen at  $-80\text{ }^{\circ}\text{C}$ . After making sections in 5  $\mu\text{m}$  thickness, samples underwent fixation in 4 % PFA for 15 minutes, then were made permeable using a blocking solution of 0.05 % Triton X-100 and 1 % BSA for 30 minutes at room temperature, followed by treating antibodies.

From antibody treating steps, all samples were treated with primary antibodies for overnight at  $4\text{ }^{\circ}\text{C}$ . Following three washes with PBS, they were exposed to secondary antibodies for an hour at room temperature. Confocal microscopy was used for image acquisition, followed by image analysis using ZEN software (V3.0, Carl-Zeiss) or Image J.

## 12. PCR

In this study, PCR was conducted using in vitro and in vivo samples. Total RNA was extracted using Trizol (15596018, Thermo Fisher), and complementary DNA synthesis was performed using AccuPower CycleScript RT premix (K2004, Bioneer, Seoul, Republic of Korea) as per the guidelines provided by the manufacturer. A real-time PCR system (StepOne V2.3, Applied Biosystems, Waltham, MA, USA) was run using SYBR green PCR mix (4367659, Applied Biosystems) with primers (Table 1). The data were

adjusted based on the expression of glyceraldehyde 3-phosphate dehydrogenase (GAPDH) using the  $2^{-\Delta Ct}$  method.

<b>Gene</b> <b>(mouse)</b>	<b>Forward (5'→3')</b>	<b>Reverse (5'→3')</b>
<b>GAPDH</b>	GGA GAG TGT TTC CTC GTC CC	ATC CGT TCA CAC CGA CCT TC
<b>CD34</b>	GAT GAA CCG TCG CAG TTG GA	GGT CTT CAC CCA GCC TTT CT
<b>SCA1</b>	GCT CAG GGA CTG GAG TGT TAC	CAG GGT AGG GGC AGG TAA TTG
<b>VE</b> <b>cadherin</b>	ATG GCA GGC CCT AAC TTT CC	TCT CTT TTG GCG ATG GTG GG
<b>VEGFR</b>	GGA AGG CCC ATT GAG TCC AA	TGG TGA GTT CAT CGC CAA CA
<b>CD31</b>	ACG AGC CCA ATC ACG TTT CA	CTT GGT GGA AGG GTC TGT CC
<b>vWF</b>	GGG ACC AAA ACG GAA GTC CA	CTG ACC CCT CCA GGA CAAAC

**Table 1.** Primers

### 13. FACS

For FACS using spleen tissues, tissues were chopped with plunger of syringe, in solution of Dulbecco's PBS (DPBS; LB001, Welgene) with 2 % FBS. The solutions were passed through 70  $\mu$ m strainer (93070, SPL), and centrifuged at 500 g for 8 minutes. Then, cells were resuspended in solution of DPBS with 2 % FBS, and 2 mM EDTA (15575-038, Invitrogen, Waltham, MA, USA), followed by incubation with antibody incubated with antibody for 1 hour at 4 °C, and were run for FACS (LSR II, BD bioscience, Mississauga, Canada).

#### 14. Statistical analysis

All statistics in this study was conducted using the Prism software (GraphPad, San Diego, CA, USA). The results are shown as the mean  $\pm$  standard error of the mean (SEM) based on more than three independent experiments. The significance of the differences between the two groups was determined using a two-tailed Student's t-test. Comparisons across various test groups were made through a one-way analysis of variance (ANOVA), with subsequent post-hoc Tukey's analysis. Statistical significance was set at  $p < 0.05$ , and expressed \* (for  $p < 0.05$ ), \*\* (for  $p < 0.01$ ), and \*\*\* (for  $p < 0.001$ ). The size of biologically independent samples per group and/or the number of independent experiments are denoted in each figure and legend, with dotted on graph for each n (when  $n \leq 10$ ).

### III. RESULTS

#### 1. Nano-hypoxia for splenic in situ reprogramming towards vasculogenic cells

##### A. The effect of hypoxia during culture of splenic mononuclear cells

To evaluate the effect of 'nano-hypoxia' on 'in situ' reprogramming in a step-by-step manner, the effect of hypoxia on in vitro cultured splenic mononuclear cells was initially investigated (**Figure 4a**). Splenic mononuclear cells were prepared using a CD11b positive selection kit since CD11b serves as a marker for mononuclear cells and these cells are known to target inflammatory sites. When these cells were cultured under hypoxic conditions, their morphology changed to a smaller and more circular shape compared to cells cultured under non-hypoxic conditions (**Figure 4b**).

The expression of the CD11b marker was found to decrease in the hypoxia group compared to the untreated group (**Figure 4c**). However, when evaluating the expression of the CD34 and SCA1 markers as vasculogenic cell markers, they were highly expressed in the hypoxia group compared to the untreated group.

Thus, these data indicate that hypoxia affected the cellular morphology and protein expression of splenic mononuclear cells, leading them towards a vasculogenic phenotype.

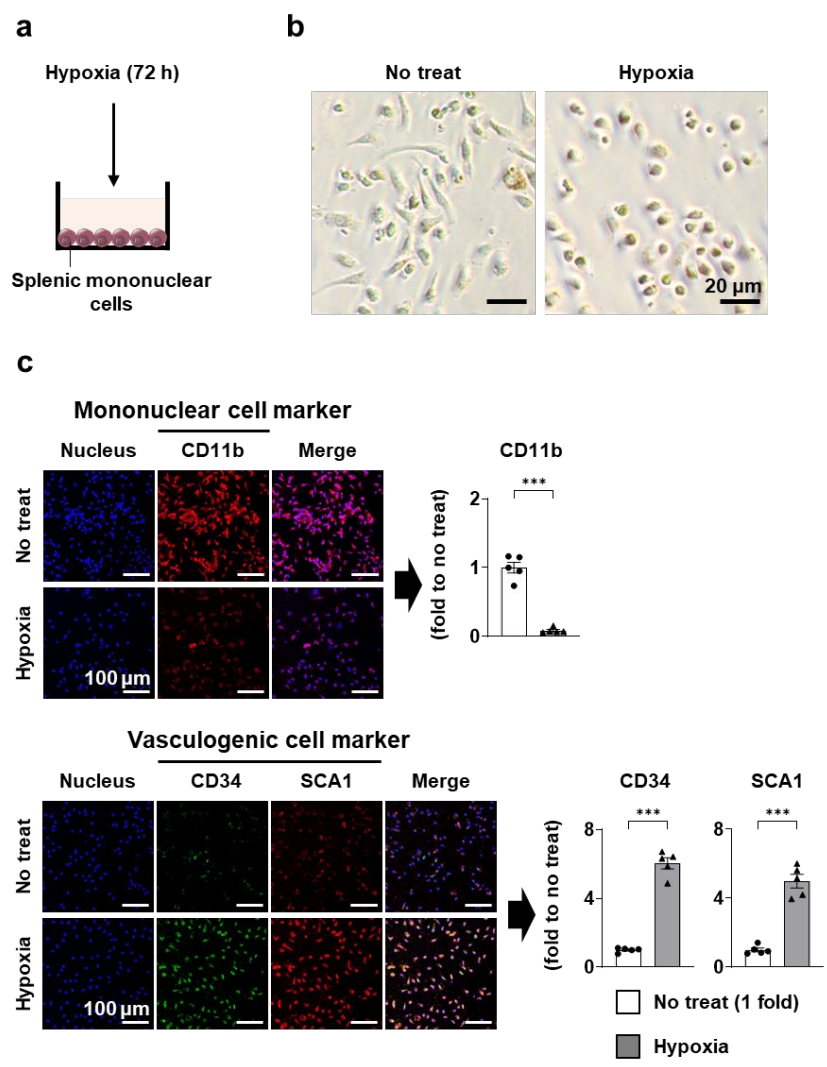


**Figure 4.** Hypoxia reprogrammed splenic mononuclear cells towards vasculogenic cells<sup>1</sup>.

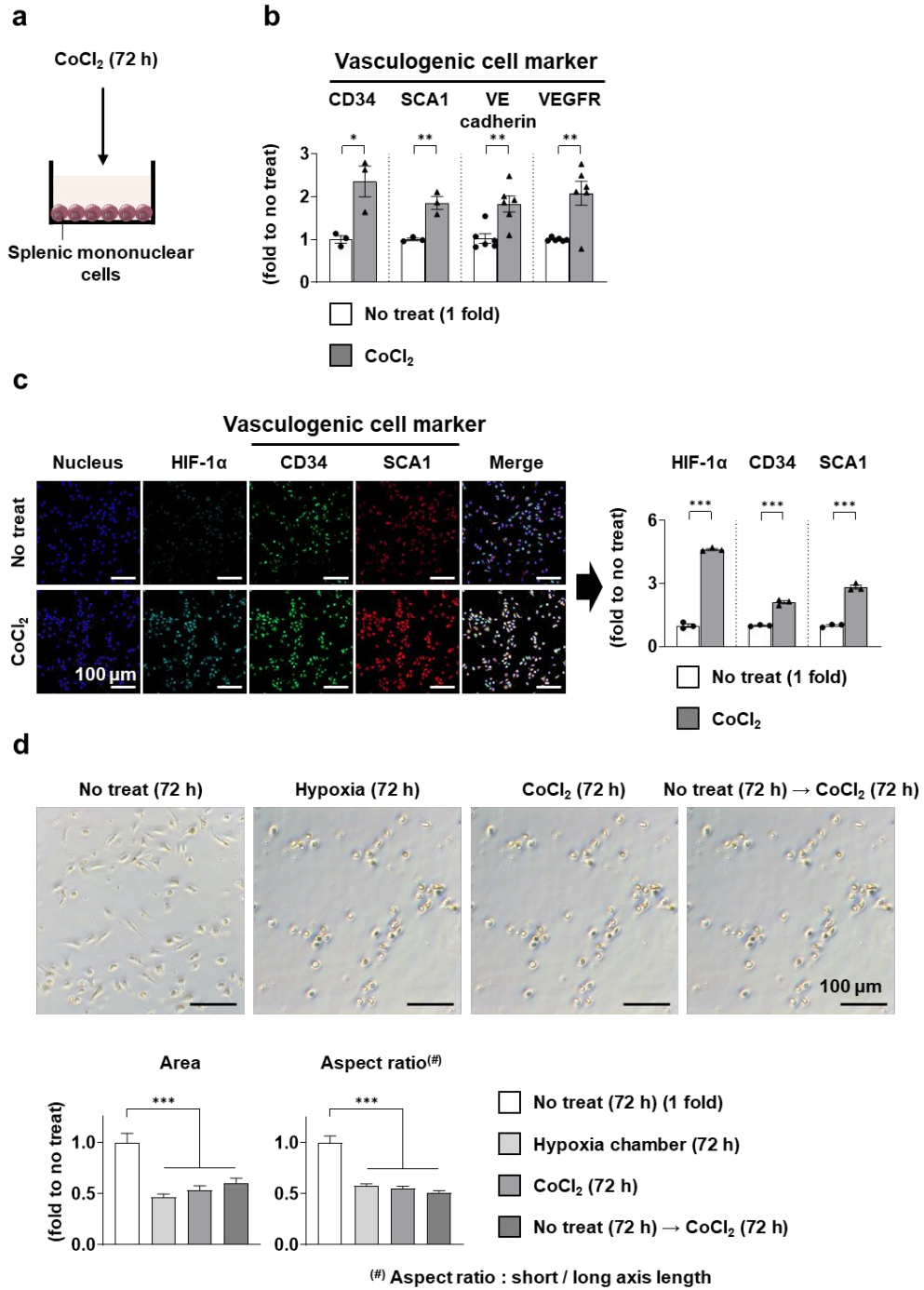
## B. The effect of a hypoxic-mimetic agent on the culture

Next, similar experiments were conducted using a hypoxic-mimetic agent instead of hypoxia (**Figure 5a**). Compared to the no treat group, the  $\text{CoCl}_2$  group showed higher gene expressions of vasculogenic cell markers, such as CD34, SCA1, VE-cadherin, and VEGF receptor (VEGFR) (**Figure 5b**). To validate that the hypoxic condition was well mimicked using  $\text{CoCl}_2$ , HIF-1 $\alpha$  expression was checked.  $\text{CoCl}_2$ -treated cells showed increased protein expression of HIF-1 $\alpha$  and, consequently, increased protein expressions of vasculogenic cell markers such as CD34 and SCA1 (**Figure 5c**).

When the effects of hypoxia and the hypoxic-mimetic agent were compared, the smaller and more circular morphology was similarly shown in both the hypoxia and  $\text{CoCl}_2$  groups compared to the no treat group (**Figure 5d**). However, the morphology of the no treat group also changed to a smaller and more circular morphology when  $\text{CoCl}_2$  was administered later. These observations were quantified in terms of area and aspect ratio, and all three groups exposed to hypoxia or the hypoxic-mimetic agent significantly showed differences in those parameters compared to the no treat group.

Vasculogenic cells are characterized by their ability to facilitate angiogenesis. Thus, an in vitro angiogenesis model was used to confirm the reprogramming of splenic mononuclear cells towards vasculogenic cells. When endothelial cells were co-cultured with pre- or post-reprogrammed cells, reprogrammed cells showed a longer tubule length with higher VEGF concentrations in the media (**Figure 5e**). The angiogenic ability of vasculogenic cells was even higher in an inflamed condition, which could be helpful since vasculogenic cells are supposed to facilitate angiogenesis after targeting an inflamed area.

In summary, the hypoxic-mimetic agent reprogrammed splenic mononuclear cells similarly to hypoxia, and the resulting vasculogenic cells showed the ability to facilitate angiogenesis.



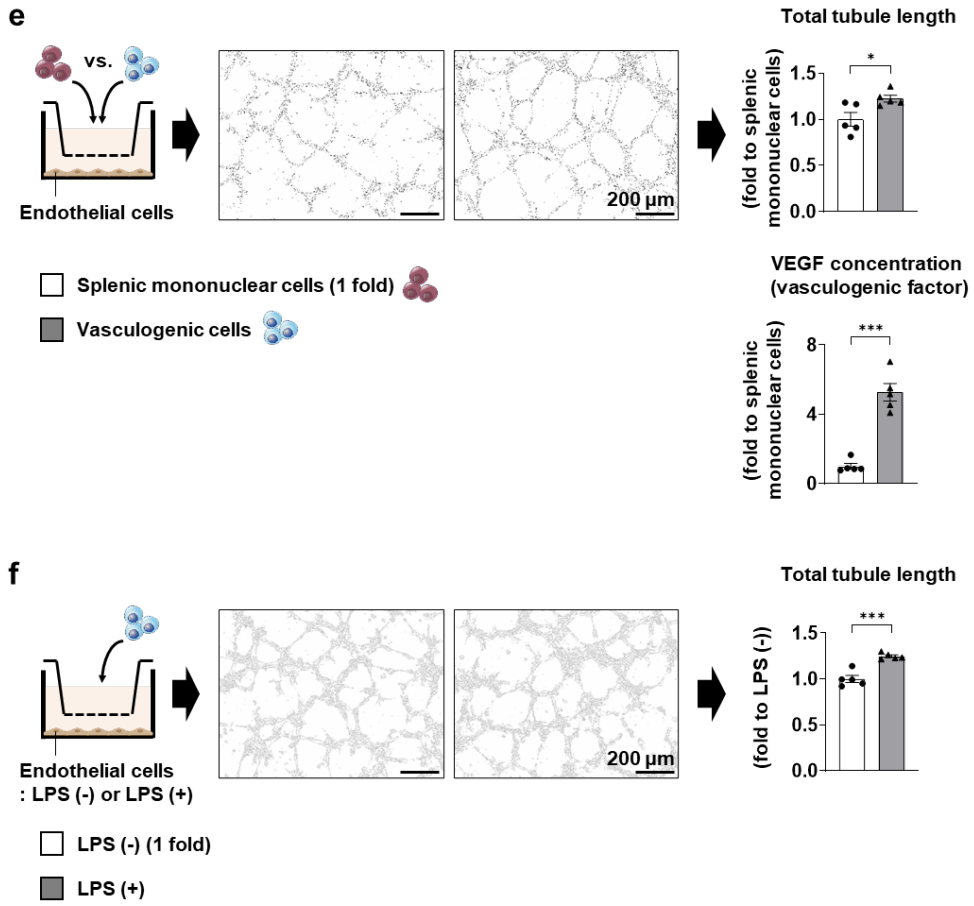


**Figure 5.** Reprogrammed vasculogenic cells by hypoxic-mimetic agent facilitate angiogenesis<sup>1</sup>.

### C. Nano-hypoxia as a vasculogenic reprogrammer of the cells

To deliver the effect of vasculogenic reprogramming effect to the splenic mononuclear cells in vivo, we coined a delivery method called ‘nano-hypoxia’. By encapsulating  $\text{CoCl}_2$  inside the liposome, the hypoxic-mimetic agent could be delivered to the spleen, and further to the splenic mononuclear cells.

Before administering nano-hypoxia in vivo, vasculogenic reprogramming effect was evaluated in in vitro culture splenic mononuclear cells (**Figure 6a**). The  $\text{CoCl}_2$ -loaded liposomes were prepared, and circular morphology with median diameter of 126 nm were confirmed using TEM and NTA, respectively (**Figure 6b-c**). When these liposomes were treated in splenic mononuclear cells, increased expressions of HIF-1  $\alpha$ , CD34, and SCA1 were checked compared to the no treat group (**Figure 6d**), which were similarly observed as the effects of hypoxia and hypoxic-mimetic agent.

So, based on  $\text{CoCl}_2$ -loaded liposomes, the nano-hypoxia could deliver the vasculogenic reprogramming effect of hypoxia to the splenic mononuclear cells.

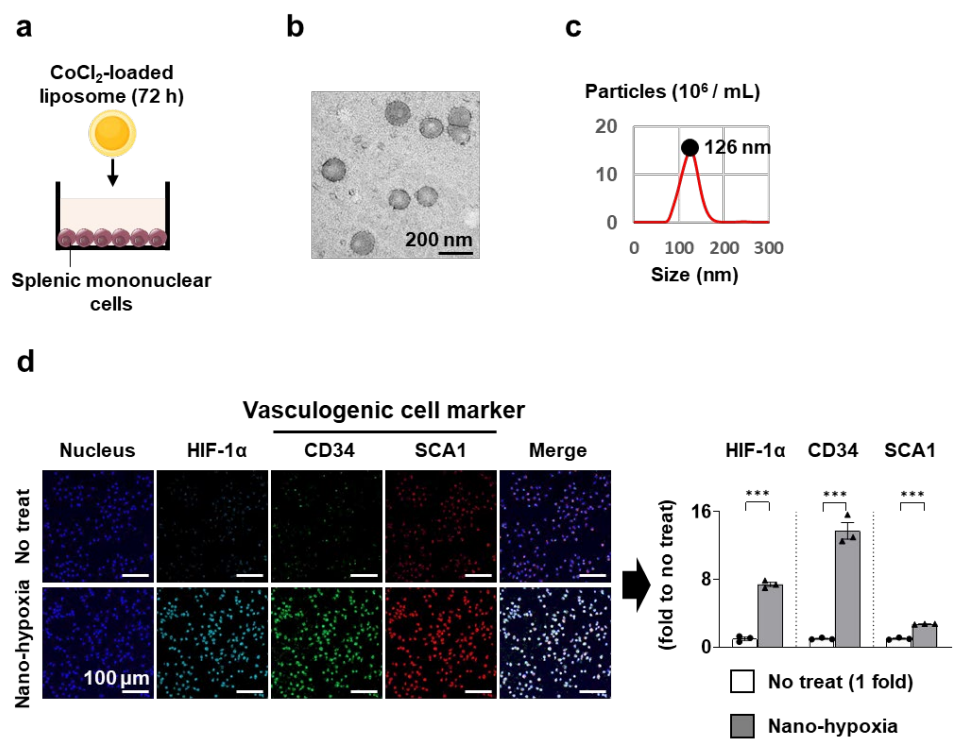


**Figure 6.** Nano-hypoxia delivers hypoxic reprogramming effect in vitro<sup>1</sup>.

#### D. In situ reprogramming strategy by nano-hypoxia in mice

For the in situ reprogramming strategy, we validated the delivery of CoCl<sub>2</sub>-loaded liposomes to the spleen and further to the splenic mononuclear cells, and the consequent vasculogenic reprogramming. When CoCl<sub>2</sub>-loaded liposomes were administered intravenously to the mouse (**Figure 7a**), the cobalt amount in the spleen significantly increased compared to the baseline (**Figure 7b**).

To further specify the destination of CoCl<sub>2</sub>-loaded liposomes inside the spleen, we used the CD11b positive selection kit. When those liposomes were administered with fluorescent tags, most of the fluorescence signals were detected in CD11b(+) cells, or splenic mononuclear cells, in comparison to significantly less uptake of those liposomes in other splenocytes (**Figure 7c**).

The uptake of liposomes in splenic mononuclear cells was also confirmed using TEM (**Figure 7d**). When gold nanoparticles were loaded on liposomes, those cargoes were found in cells of the red pulp area, indicated by the existence of red blood cells (RBCs), also known as the mononuclear cell reservoir of the spleen. Also, when mononuclear cells were specified by the ratio of nuclear and cytoplasm, gold nanoparticles were found in those cells.

Consequently, the delivery of vasculogenic reprogramming effect was also validated. Compared to the no treat group, the nano-hypoxia group showed decreased mononuclear cell markers such as CD11b, and increased vasculogenic cell markers such as CD34 and SCA1 (**Figure 7e**).

Thus, nano-hypoxia can be used to deliver hypoxic-mimetic agents to the splenic mononuclear cells and subsequently turn them vasculogenic, as planned for the in situ reprogramming strategy.

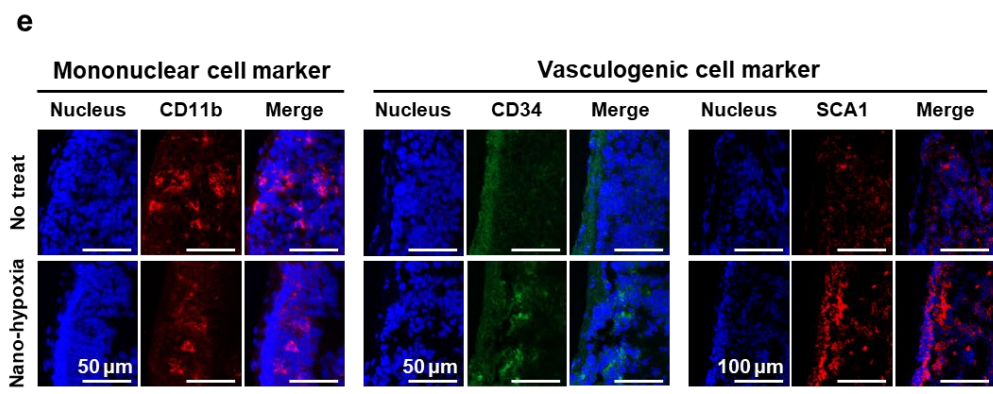
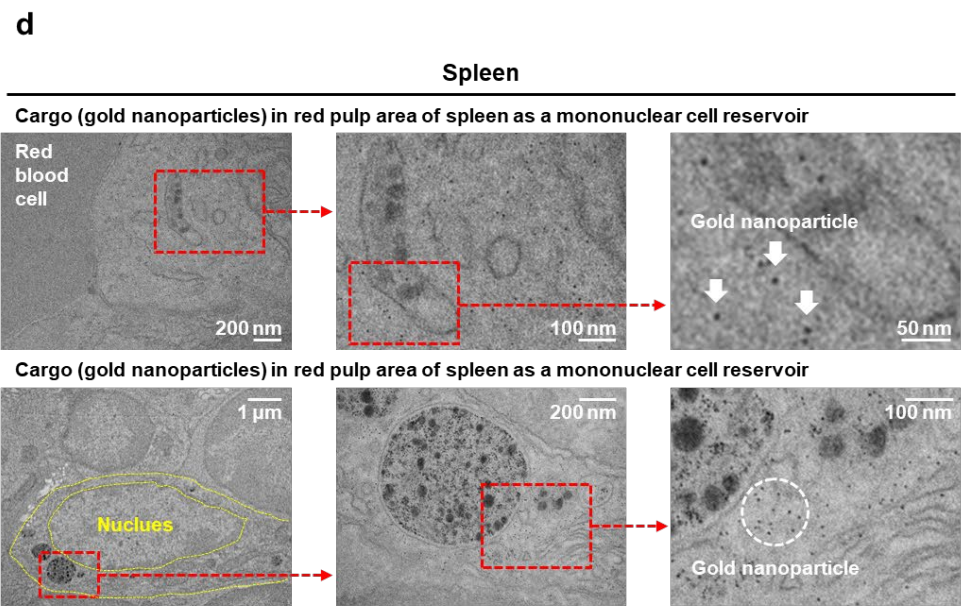
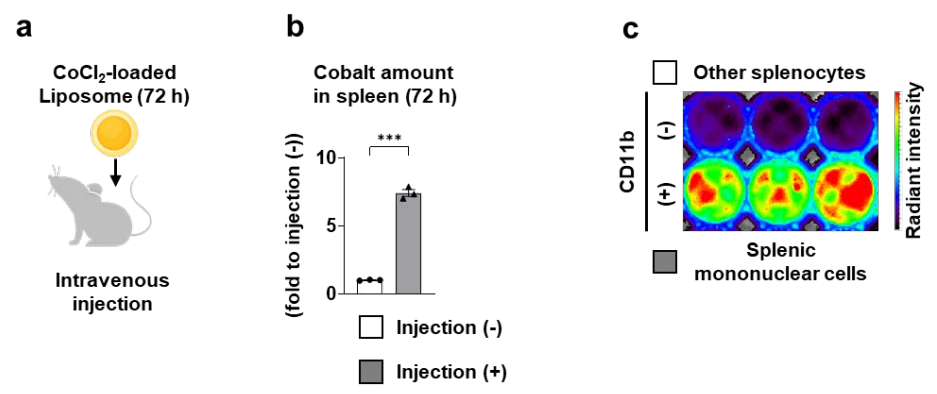


**Figure 7.** Nano-hypoxia delivers hypoxic reprogramming effect in vivo<sup>1</sup>.

#### E. Validation of the reprogramming effect

To validate the vasculogenic reprogramming effect of nano-hypoxia, we compared the effects of nano-hypoxia with actual hypoxic conditioning on the spleen. The splenic artery was surgically ligated, and the color change of the spleen was shown just after the ligation as proof of hypoxic conditioning (**Figure 8a**).

In the results, both the nano-hypoxia group and the splenic artery ligation group showed decreased mononuclear cell markers such as CD11b and CD45, and increased vasculogenic cell markers such as CD34 and VE-cadherin, compared to the no treat group (**Figure 8b**). There were some differences in the reduction level of CD11b in the two hypoxic groups, but they showed similar tendencies in the expressions of all markers.

Thus, similar to the comparable vasculogenic reprogramming effect of hypoxia and the hypoxic-mimetic agent on splenic mononuclear cells, nano-hypoxia and splenic artery ligation also showed comparable vasculogenic reprogramming effects on the spleen.

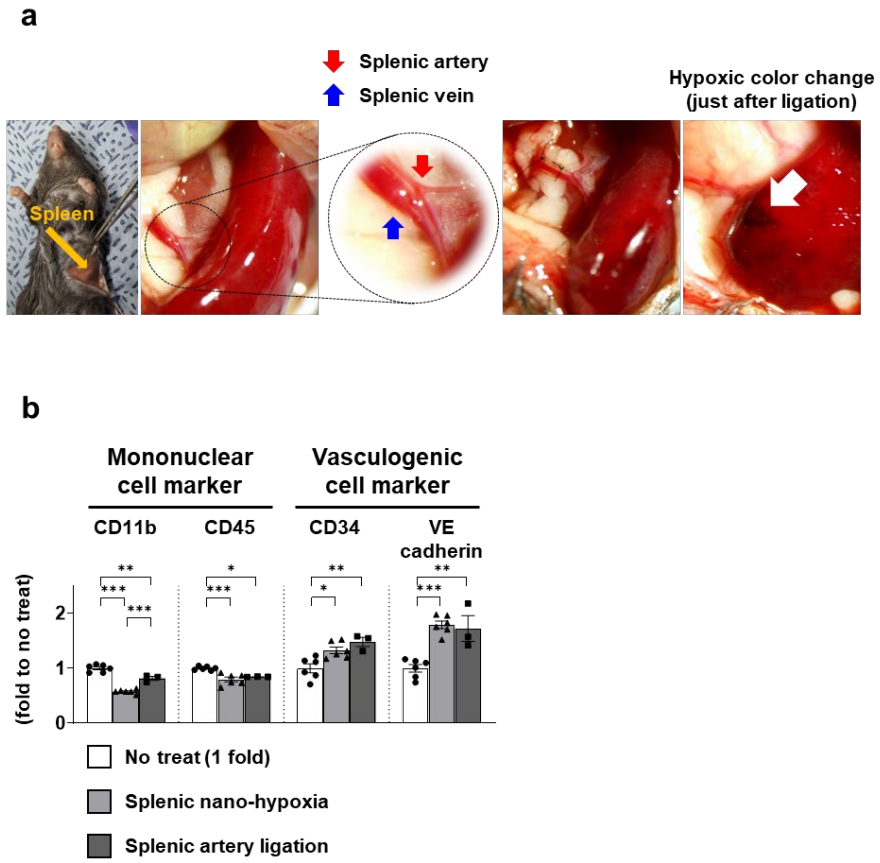


**Figure 8.** Validation of hypoxic reprogramming effect of nano-hypoxia<sup>1</sup>.

#### F. Secured vasculogenic cell amounts in the strategy

As mentioned earlier, one of the possible limitations of the conventional strategy was the insufficient dose of vasculogenic cells. Therefore, we evaluated the therapeutic efficacy of the in situ reprogramming strategy by ensuring an adequate number of vasculogenic cells using nano-hypoxia.

Compared to the bone marrow cells used in the conventional strategy, the percentage of vasculogenic marker-positive cells, such as CD34, VE-cadherin, and c-Kit, was higher in splenic cells under nano-hypoxia (**Figure 9a**). Furthermore, we compared the absolute cell numbers of vasculogenic marker-positive cells to the conventional strategy's dose, which typically involves 500,000 CD34(+) cells. The splenic cells under nano-hypoxia exhibited more than a 20-fold increase in CD34(+) cells compared to the conventional strategy dose and a 10-fold increase compared to bone marrow cells (**Figure 9b**).

In conclusion, the in situ reprogramming strategy demonstrated a clear advantage in securing vasculogenic cell amounts, being 20-fold higher than the conventional strategy dose and 10-fold higher than bone marrow cells.

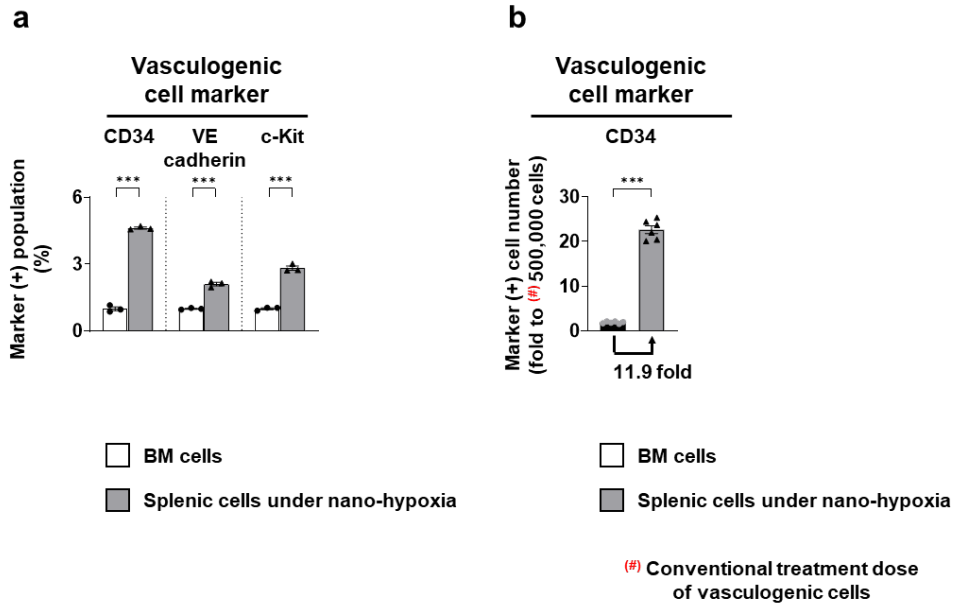


**Figure 9.** Advantage in vasculogenic cell amounts of in situ reprogramming<sup>1</sup>.

## 2. Spleen-mediated targeting even after the reprogramming

### A. 3D chip model

The aforementioned results proved the reprogramming of splenic mononuclear cells towards vasculogenic cells, which showed different degrees of marker expressions and angiogenesis facilitation between the two cell groups. However, this change may affect the inflammatory site targeting ability of splenic mononuclear cells, which is critical for spleen-mediated targeting.

The 3D chip model was used to assess the inflammatory site targeting ability of reprogrammed vasculogenic cells (**Figure 10a**). Tissues from the ischemic hindlimb and contralateral hindlimb were collected as models of target sites with or without inflammation. These tissues were ex vivo cultured in a 3D hydrogel chip with media perfusion through a microchannel network inside the chip. The tissues can be kept alive in this system for more than 24 hours (**Figure 10b**).

Next, reprogrammed vasculogenic cells were seeded between the two tissues, and the migration of the cells was imaged. Significantly more cells targeted the tissue with inflammation compared to that without inflammation, as quantified to more than a 2-fold degree.

These results showed that reprogrammed vasculogenic cells still possess the ability to target inflammatory sites.

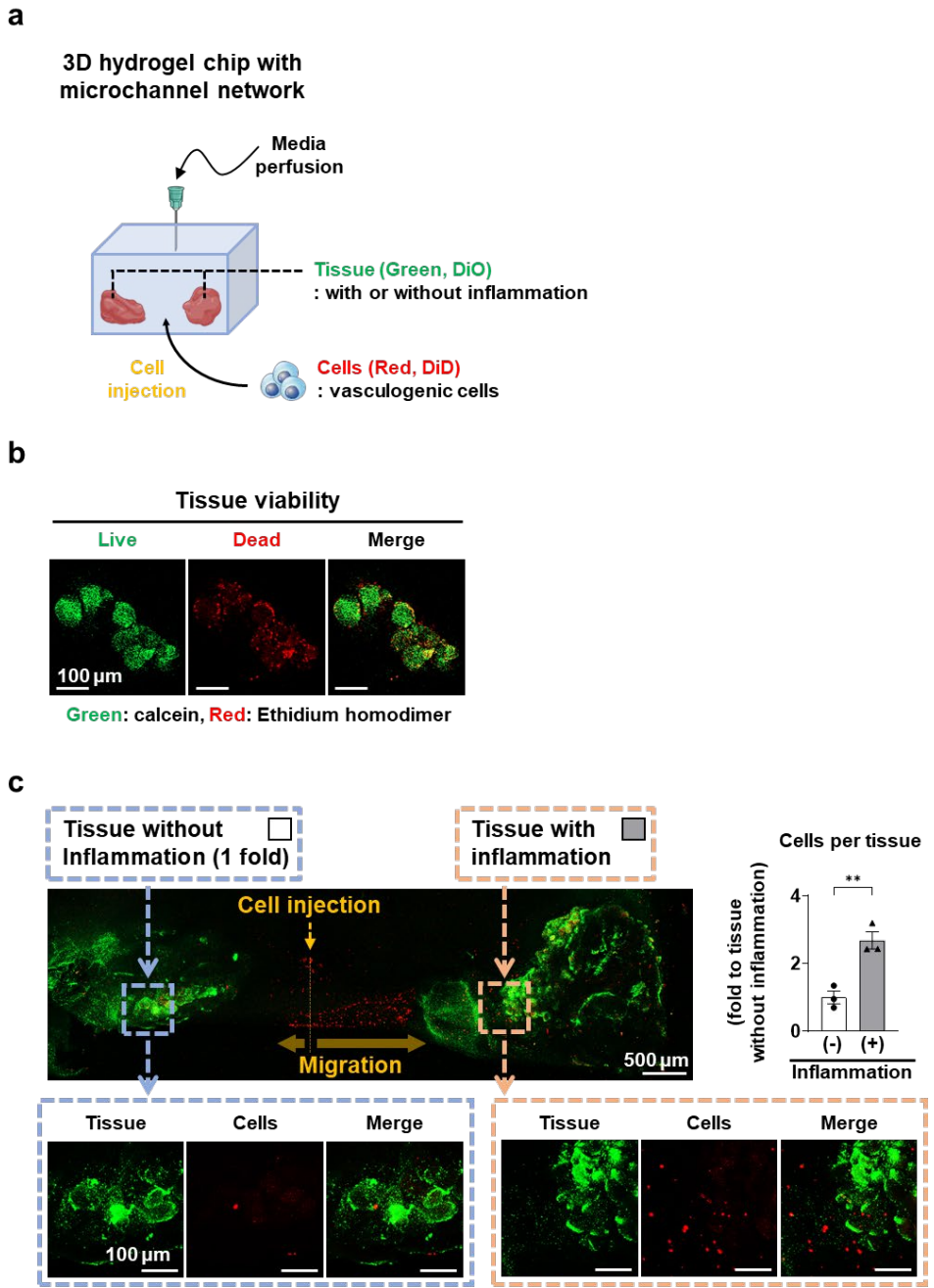


Figure 10. Targeting of vasculogenic cells in 3D chip model<sup>1</sup>.

## B. In vivo models

To validate the spleen-mediated targeting in the in situ reprogramming strategy, hindlimb ischemia was induced in mice as a target site under inflammation (**Figure 11a**). After administering CoCl<sub>2</sub>-loaded liposomes tagged with fluorescence or <sup>19</sup>F, hindlimb ischemia was induced, followed by evaluating the distribution of those liposomes.

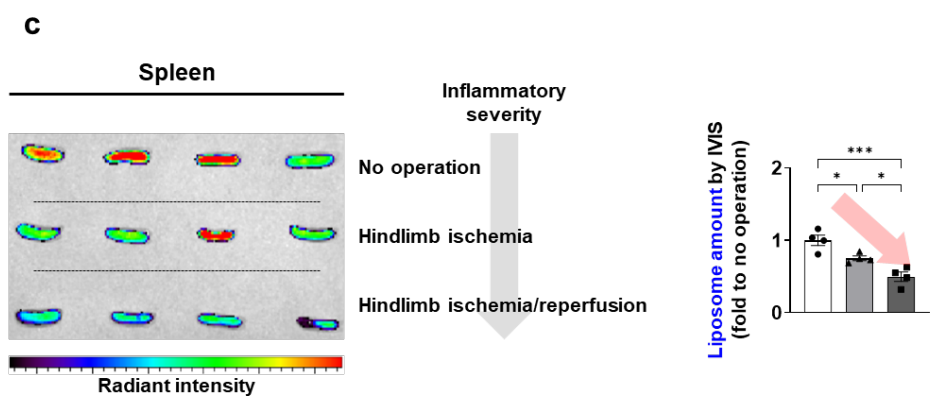
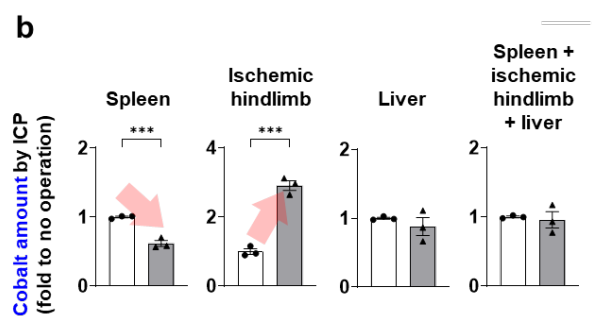
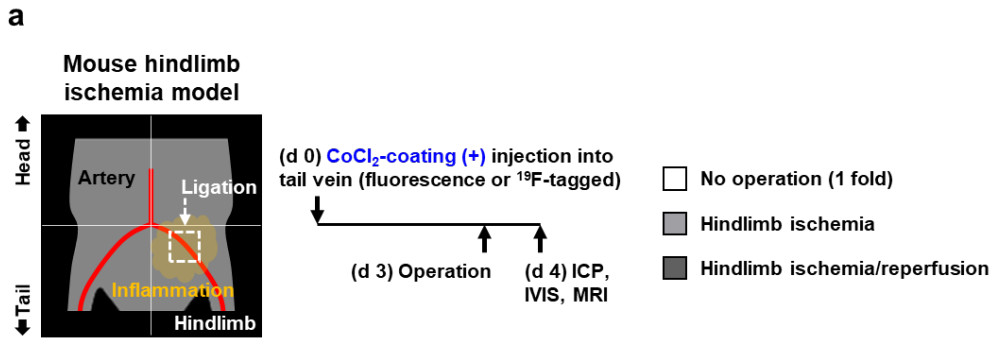
When the liposomes were tracked by cobalt amount, the aforementioned increased cobalt amount in the spleen decreased in the hindlimb ischemia group compared to the no operation group (**Figure 11b**). In contrast, the cobalt amount in the ischemic hindlimb increased to about 3-fold after hindlimb ischemia induction compared to the baseline. These results indicate that some of the cobalt in the spleen moved to the ischemic hindlimb by hindlimb ischemia induction. However, whether hindlimb ischemia was induced or not, the cobalt amount in the liver or the total cobalt amount in the spleen, ischemic hindlimb, and liver did not change. Thus, the cobalt from the spleen was the major portion of the increased cobalt in the ischemic hindlimb, rather than from the liver or any other organs.

Furthermore, the decrease in the cobalt amount in the spleen was evaluated by inducing a different degree of inflammatory induction. Reperfusion after inducing ischemia in the hindlimb is known to paradoxically induce more severe damage compared to ischemia without perfusion. Compared to the no operation group, the amount of fluorescence-tagged liposomes in the spleen was decreased in the hindlimb ischemia group, but even more significantly decreased in the hindlimb ischemia/reperfusion group (**Figure 11c**). This means that a severe degree of inflammation induces more spleen-mediated targeting.

To evaluate the geographical distribution of spleen-mediated targeting around the inflammatory sites, MRI was used to track the liposomes tagged with <sup>19</sup>F by encapsulating perfluorohexanol inside the liposomes. The resulting liposomes showed a similar chemical shift with perfluorohexanol (**Figure 11d**). When the <sup>19</sup>F signals

were tracked, the strongest signals were found at the ligation site of the artery, and the signals weakened as they spread out from there. Also, there were no signals in the contralateral hindlimb as no inflammation was induced.

In summary, the inflammatory site targeting could be achieved even after reprogramming splenic mononuclear cells. The spleen plays a major role in that targeting, and the amount of targeting is relative to the degree of inflammation.



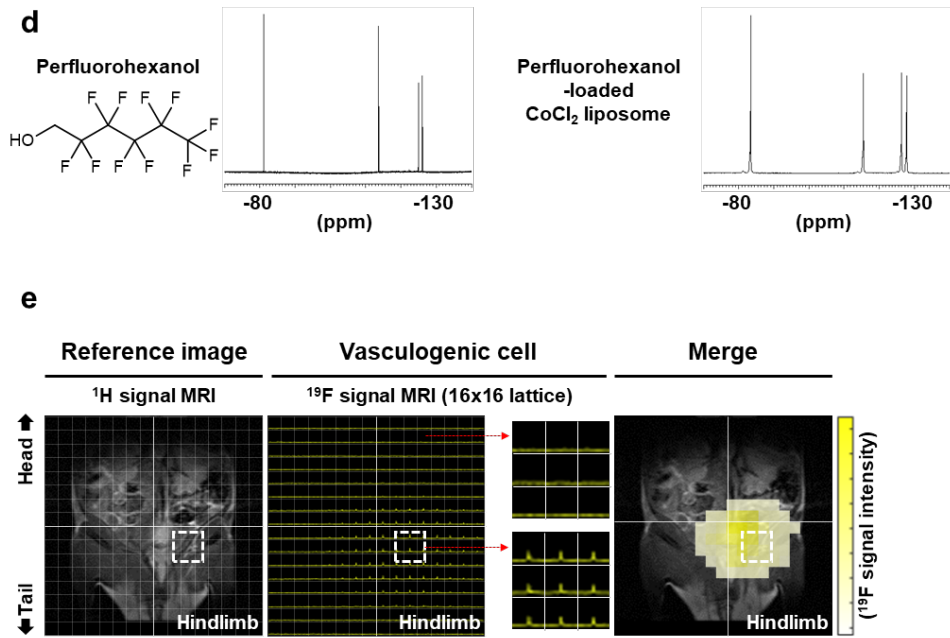


**Figure 11.** Targeting of vasculogenic cells in in vivo models<sup>1</sup>.

### 3. Therapeutic efficacy in preclinical models

#### A. Mouse hindlimb ischemia model

The mouse hindlimb ischemia model was used to evaluate the facilitation of angiogenesis by vasculogenic cells reprogrammed by nano-hypoxia (**Figure 12a**). In the nano-hypoxia group,  $\text{CoCl}_2$ -loaded liposomes were intravenously injected into the mice, and hindlimb ischemia was induced three days later. For comparison with the conventional strategy, bone marrow cells were directly injected into the ischemic sites just after the induction of hindlimb ischemia. All mice were evaluated for angiogenesis, blood flow recovery, and biosafety over a period of two weeks after the surgery.

The nano-hypoxia group exhibited increased cell invasion into the ischemic hindlimb in H&E staining, and increased angiogenic markers such as CD31 and vWF in immunofluorescence staining, compared to the no treat group (**Figure 12b**). The conventional strategy group also showed increased angiogenesis in H&E and immunofluorescence staining compared to the no treat group, but the levels were significantly lower than those in the nano-hypoxia group. Same trends were observed in gene expressions of those angiogenic markers (**Figure 12c**).

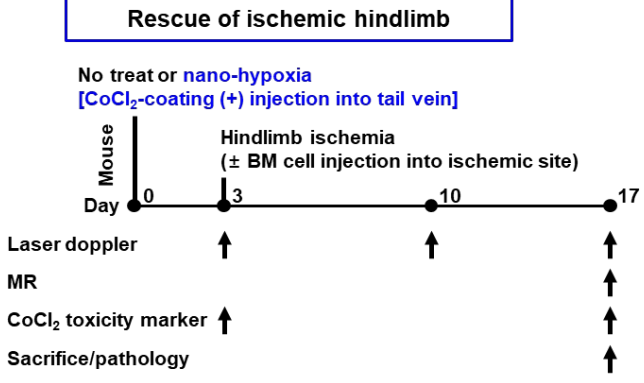
Next, the blood flow recovery subsequent to the angiogenesis was evaluated. When each mouse underwent repeated laser doppler imaging, the nano-hypoxia group showed significantly higher blood flow compared to the no treat group during the two-week follow-up (**Figure 12d**). The conventional strategy group exhibited similar levels of blood flow recovery as the nano-hypoxia group in the first week, but it fell below the levels of the nano-hypoxia group in the second week.

Blood flow recovery was further evaluated using MRI (**Figure 12e**). In 2D MRI, the nano-hypoxia group showed increased contrast signal in the ischemic hindlimb compared to the other groups. This tendency was maintained in 3D MRI, which exhibited a high signal in the nano-hypoxia group.

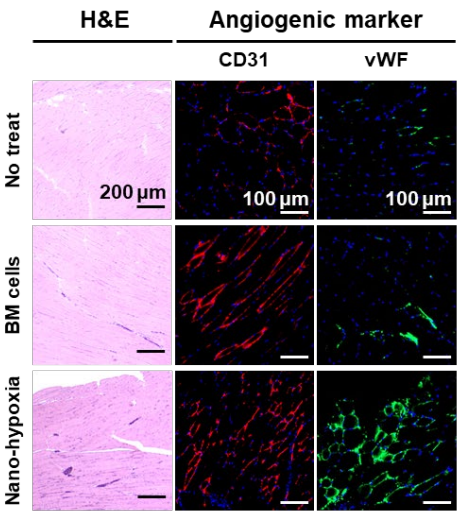
In summary, the in situ reprogramming by nano-hypoxia demonstrated therapeutic

efficacy in facilitating angiogenesis and blood flow recovery. Furthermore, the effects of the in situ reprogramming showed superiority compared to the conventional strategy.

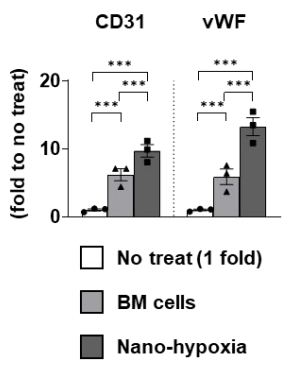
**a**



**b**



**c**



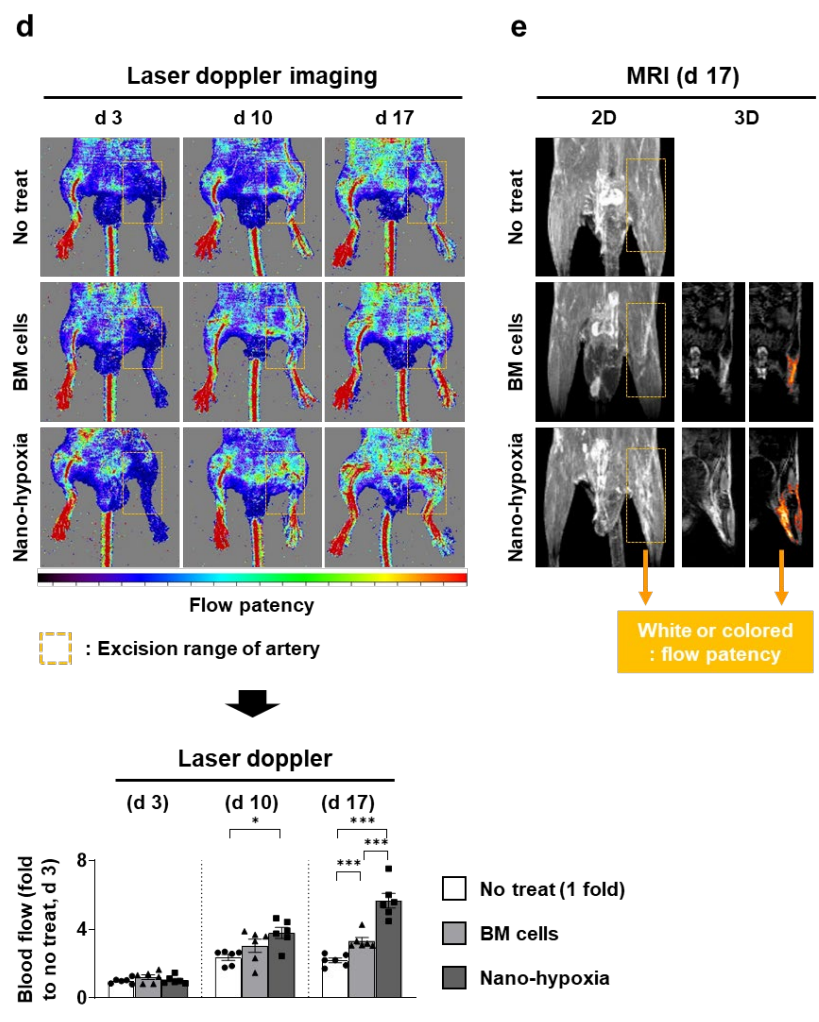


**Figure 12.** In situ reprogramming in mouse hindlimb ischemia model<sup>1</sup>.

## B. Biosafety of nano-hypoxia

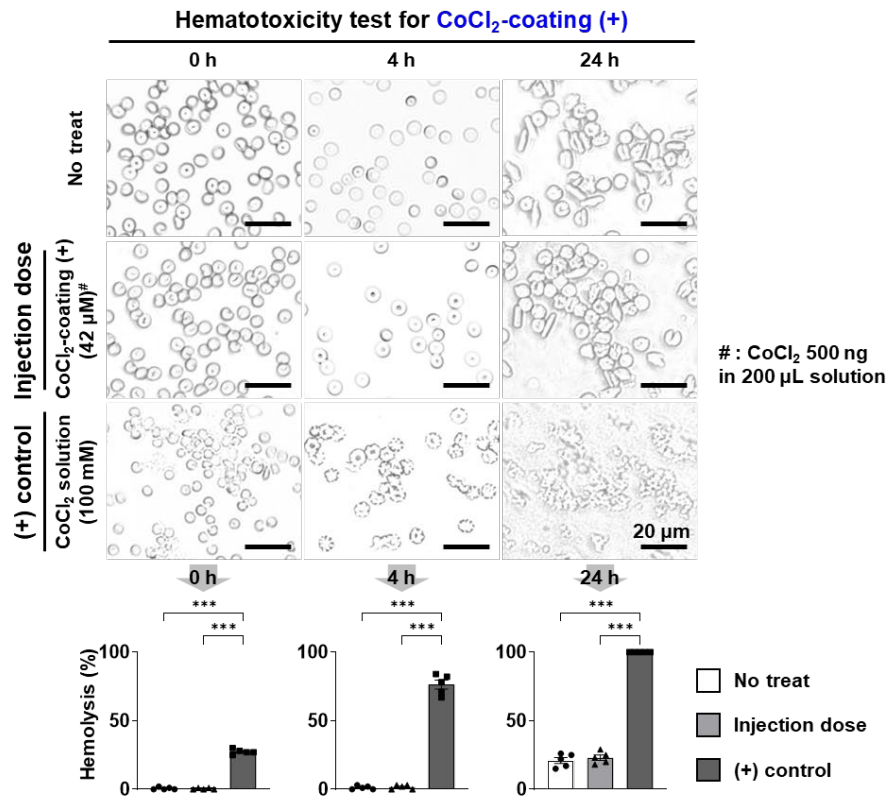
To apply the in situ reprogramming strategy in clinical settings, possible off-target effects of nano-hypoxia were evaluated. After administration through intravenous injections, CoCl<sub>2</sub>-loaded liposomes primarily distributed to the liver and spleen. Thus, the blood and liver are the major organs that encounter CoCl<sub>2</sub>-loaded liposomes.

Hematotoxicity of CoCl<sub>2</sub>-loaded liposomes was assessed by incubating RBCs with these liposomes (**Figure 13a**). When positive control groups were prepared with a high concentration of CoCl<sub>2</sub>, RBCs started to undergo hemolysis immediately after co-incubation began, and most of the RBCs were hemolyzed within 24 hours. However, the injection dose of CoCl<sub>2</sub>-loaded liposomes showed significantly less hemolysis compared to the positive control group and was similar to the no treat group.

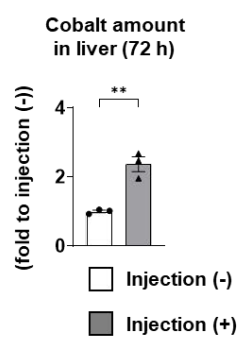
Hepatotoxicity of nano-hypoxia was evaluated since the injection of CoCl<sub>2</sub>-loaded liposomes resulted in a more than 2-fold increase in cobalt amount in the liver (**Figure 13b**). However, when hepatocyte enzymes in the serum were assessed as a marker of hepatotoxicity, there were no significant differences between the groups that received CoCl<sub>2</sub>-loaded liposomes and the groups that did not receive them (**Figure 13c**).

Thus, there were no significant off-target effects in the majorly distributed organs after the intravenous injection of CoCl<sub>2</sub>-loaded liposomes.

**a**



**b**



**c**

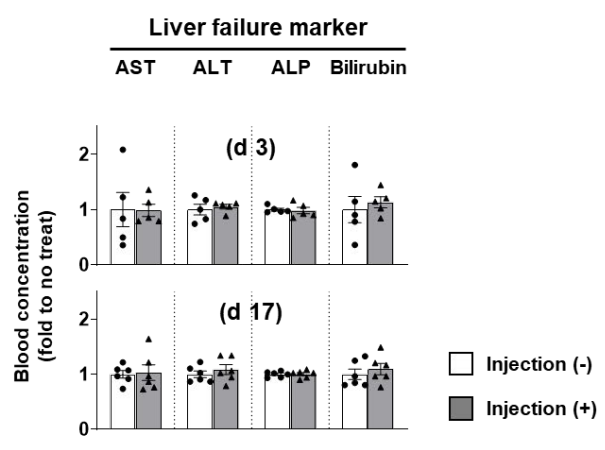


**Figure 13.** Biosafety of nano-hypoxia<sup>1</sup>.

### C. Mouse 70 % hepatectomy model

Since angiogenesis is one of the key factors in liver regeneration after hepatectomy, facilitated angiogenesis was evaluated in a mouse 70 % hepatectomy model (**Figure 14a**). In the nano-hypoxia group, CoCl<sub>2</sub>-loaded liposomes were intravenously injected into the mice, and 70 % hepatectomy was conducted three days later. Furthermore, some mice underwent splenectomy during the hepatectomy procedures to confirm the role of the spleen in the therapeutic effect, named as the nano-hypoxia + splenectomy group. All mice were evaluated for angiogenesis and liver regeneration for four days after the surgery.

After the 70 % hepatectomy, the liver volume clearly decreased compared to the liver volume before surgery (**Figure 14b**). When angiogenic markers such as CD31, vWF, and VEGF were compared in immunofluorescence staining, the nano-hypoxia group showed increased expression of those markers compared to the no treat group, both on day 5 and 7 (**Figure 14c**). However, this effect of facilitated angiogenesis disappeared in the nano-hypoxia + splenectomy group. This indicates the major role of the spleen in this in situ reprogramming strategy.

Next, subsequent liver regeneration was evaluated in each group. The mitotic cells were counted in H&E staining as a marker of hepatocyte proliferation, and the nano-hypoxia group showed significantly more mitotic cells compared to the other groups (**Figure 14d**). This was further confirmed using Ki-67 to mark the proliferative hepatocytes (**Figure 14e**). The same trend was observed in Ki-67 staining, which was higher in the nano-hypoxia group compared to the other groups.

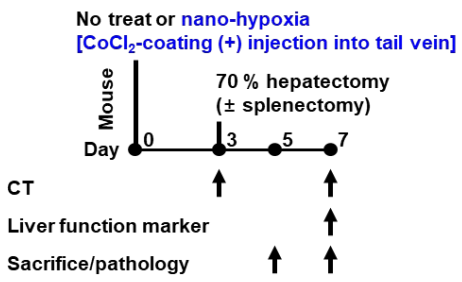
Enhanced liver regeneration in the nano-hypoxia group was further validated by liver volume, weight, and function. The decreased liver volume after hepatectomy remained unchanged in the no treat group but showed significant restoration in the nano-hypoxia group (**Figure 14f**). The average liver weight in the nano-hypoxia group was more than 2-fold higher compared to the no treat group (**Figure 14g**). Lastly, liver function was also improved due to enhanced liver regeneration in the nano-hypoxia group, as

bilirubin concentration was significantly lower in this group (**Figure 14h**).

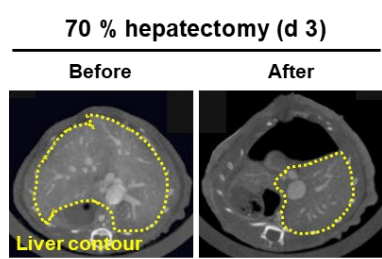
In summary, in situ reprogramming by nano-hypoxia showed therapeutic efficacy in facilitated angiogenesis and liver regeneration. Additionally, it was demonstrated that this effect was spleen-dependent.

**a**

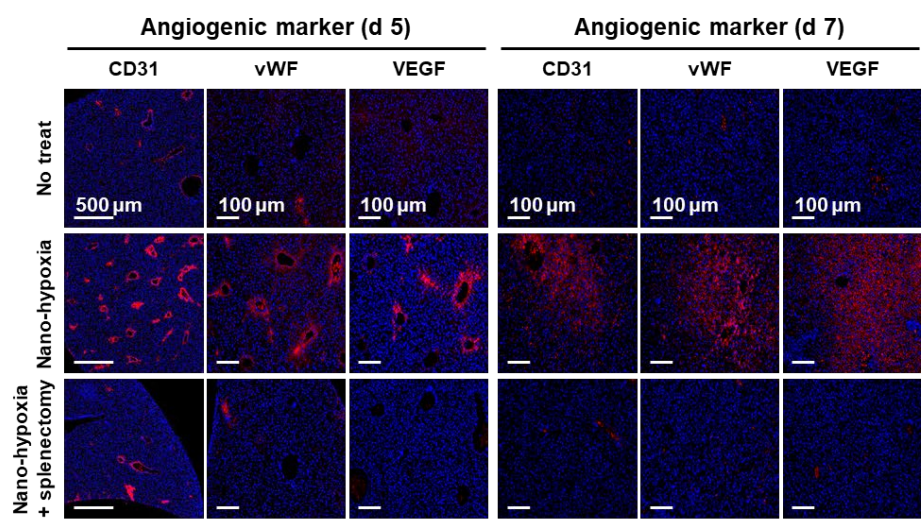
**Liver regeneration post hepatectomy**



**b**



**c**



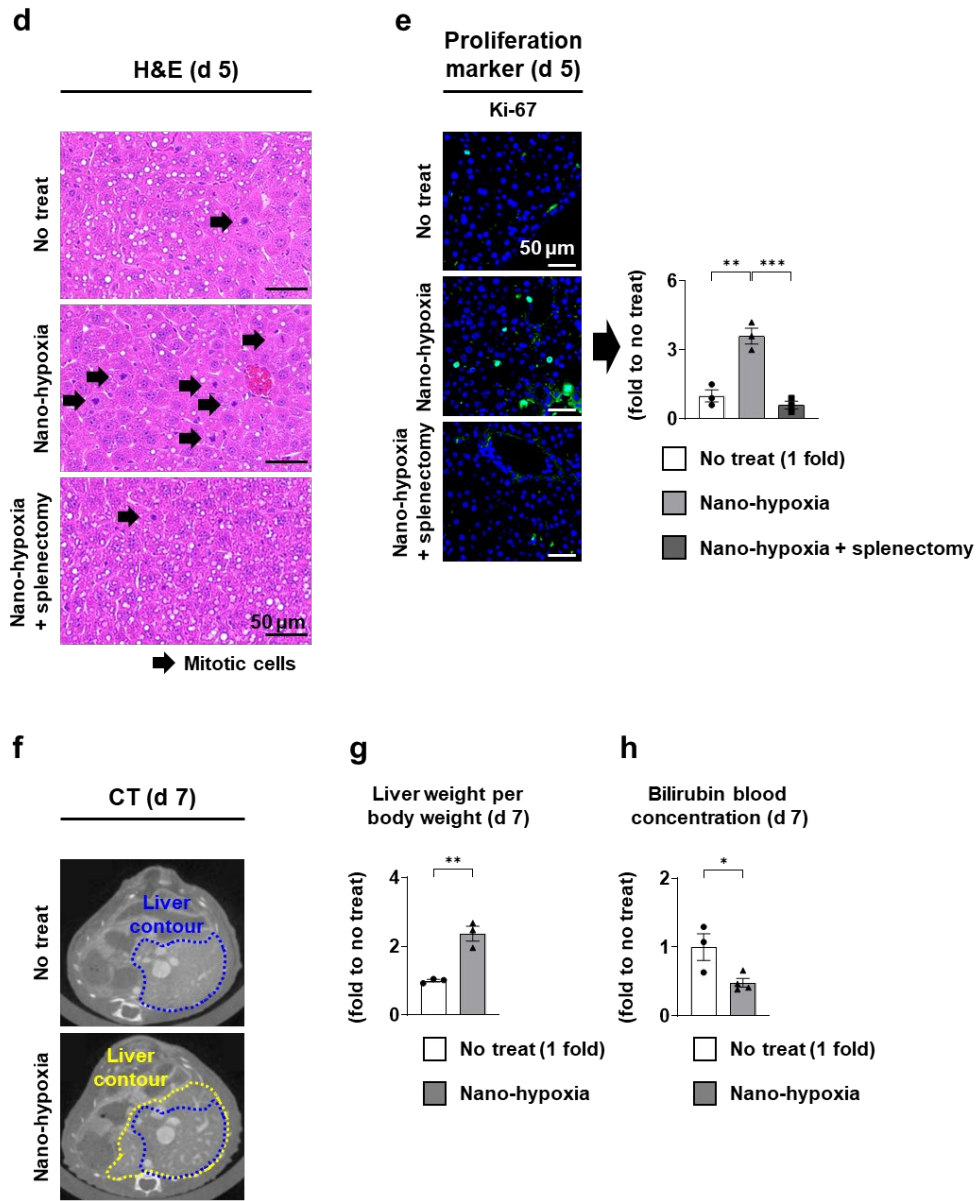


**Figure 14.** In situ reprogramming in mouse 70 % hepatectomy model<sup>1</sup>.

#### IV. DISCUSSION

Vasculogenic cell treatment can be a clinically beneficial and potent therapeutic modality, as demonstrated by constant clinical trials involving thousands of patients despite the marginal results. As proposed in this study, the in situ reprogramming strategy by nano-hypoxia can be a superior approach to the conventional one since it addresses some current unmet needs.

The first point of improvement comes with the delivery issues. Conventional treatment was set in an autotransplantation setting, which requires extraction and re-injection steps. Under these circumstances, the maximum amount of extraction is necessarily limited, requiring a lot of time and labor, not to mention the thrombotic and bleeding risks during those processes.

The in situ reprogramming strategy modifies the conventional autotransplantation setting of vasculogenic cell treatment, and all the steps are proceeded in vivo. Vasculogenic cells are prepared by delivering a priming agent by reversely using the nanoparticle capture of mononuclear cells. Migration of these cells also relies on inherent targeting to the inflammatory sites, which is hardly lost even after the vasculogenic reprogramming. It's an obviously simple and necessarily non-invasive version of vasculogenic cell treatment.

This first point also leads to the second advantage point, which is the dosing issues. Bone marrow is a popular source for mononuclear cells, and easy extractability is one major reason. Bone marrow can be a decent candidate since it generates mononuclear cells, but warehouse stores more goods compared to the factory in general. As the spleen serves as a mononuclear cell reservoir of the body, splenic mononuclear cells can be utilized without extraction.

As demonstrated in this study, nano-hypoxia can prepare a large amount of vasculogenic cells, which is 20-fold higher than the conventional treatment dose, and 10-fold higher than bone marrow cells. Furthermore, these prepared cells are automatically

distributed to the sites in need, based on an inflammatory-degree-dependent way. The therapeutic dose will be self-controlled by disease severity, and when the disease gets abruptly aggravated in progress, more dose prepared at the spleen can be delivered to the target sites.

We validated this strategy in 2 preclinical models related to angiogenesis. In our experimental settings, it has been proven that the spleen plays a major role in this treatment, and the therapeutic efficacy is superior to the conventional strategy. However, longer observations will be warranted, with careful monitoring of possible off-target effects.

Specifically, cobalt toxicity can be caused by the injection of  $\text{CoCl}_2$ -loaded liposomes, leading to effects such as oxidative stress and genotoxicity<sup>99-101</sup>. In our strategy, the cobalt level was approximately  $25 \mu\text{m/kg}$  in mouse, which is well below the toxic range of  $500 - 4,000 \mu\text{m/kg}$ <sup>99-101</sup>. This suggests a reduced likelihood of off-target cobalt toxicity. However, monitoring is recommended for repeated injections over an extended period.

Also, wider applications can be considered similar to this strategy. Vasculogenic cell treatment can be applied to many other diseases requiring tissue regeneration, such as the liver, lung, and neurons. The advantages in dose and delivery issues can be applied intact for use in those diseases, so further studies could investigate those applications.

Apart from the applications of vasculogenic cell treatment, spleen-mediated targeting can also be widely used. Splenic mononuclear cells have great potential to be reprogrammed into many other cell types, especially blood circulation cells. For example, mononuclear cells can also be reprogrammed to red blood cells. Considering the abundant amount of stored cells in the spleen, these cells could be reprogrammed to treat anemia.

The targeting efficiency of spleen-mediated targeting is also warranted for further studies. The in situ reprogramming strategy exhibited a superior therapeutic effect in addressing the dose issues compared to the conventional strategy. Still, large portions of the nanoparticles are deprived of the liver and other organs rather than the spleen, and

the targeting efficiency is hard to evaluate since only the necessary portion of the reprogrammed cells moves to the target regions.

Concentrating more targeting on the spleen can be achieved by several methods regarding nanoparticle designs, such as lipid composition, particle size, and shape. These methods will further improve the in situ reprogramming strategy in this study. Also, it's not clear whether the mononuclear cells in the liver can participate in these in situ reprogramming strategies. Hepatic mononuclear cells, such as Kupffer cells, are major populations of nanoparticle uptake, so it could also be a good strategy to utilize hepatic mononuclear cells.

## V. CONCLUSION

In situ reprogramming by nano-hypoxia of spleen is an original, and effective therapeutic strategy, validated in multiple preclinical models. It showed its superiority on facilitating angiogenesis and subsequent flow recovery or tissue regeneration, and that could be because this strategy address the dose and delivery limitations of the conventional strategy. Further studies are warranted regarding the minimizing off-target effect and optimization for the best therapeutic effect.

## REFERENCES

1. Chung S, Kim SY, Lee K, Baek S, Ha H-S, Kim D-H, et al. In Situ Reprogrammings of Splenic CD11b+ Cells by Nano-Hypoxia to Promote Inflamed Damage Site-Specific Angiogenesis. *Advanced Functional Materials* 2023;33:2302817.
2. Wilhelm S, Tavares AJ, Dai Q, Ohta S, Audet J, Dvorak HF, et al. Analysis of nanoparticle delivery to tumours. *Nature Reviews Materials* 2016;1:16014.
3. Peer D, Margalit R. Tumor-targeted hyaluronan nanoliposomes increase the antitumor activity of liposomal Doxorubicin in syngeneic and human xenograft mouse tumor models. *Neoplasia* 2004;6:343-53.
4. van Vlerken LE, Duan Z, Little SR, Seiden MV, Amiji MM. Biodistribution and pharmacokinetic analysis of Paclitaxel and ceramide administered in multifunctional polymer-blend nanoparticles in drug resistant breast cancer model. *Mol Pharm* 2008;5:516-26.
5. Shi J, Xiao Z, Kamaly N, Farokhzad OC. Self-assembled targeted nanoparticles: evolution of technologies and bench to bedside translation. *Acc Chem Res* 2011;44:1123-34.
6. Cui Y, Zhang M, Zeng F, Jin H, Xu Q, Huang Y. Dual-Targeting Magnetic PLGA Nanoparticles for Codelivery of Paclitaxel and Curcumin for Brain Tumor Therapy. *ACS Appl Mater Interfaces* 2016;8:32159-69.
7. Rosenblum D, Joshi N, Tao W, Karp JM, Peer D. Progress and challenges towards targeted delivery of cancer therapeutics. *Nat Commun* 2018;9:1410.
8. Mitchell MJ, Billingsley MM, Haley RM, Wechsler ME, Peppas NA, Langer R. Engineering precision nanoparticles for drug delivery. *Nat Rev Drug Discov* 2021;20:101-24.
9. Illum L, Davis SS. The organ uptake of intravenously administered colloidal particles can be altered using a non-ionic surfactant (Poloxamer 338). *FEBS Lett* 1984;167:79-82.
10. Moghimi SM, Porter CJ, Muir IS, Illum L, Davis SS. Non-phagocytic uptake of intravenously injected microspheres in rat spleen: influence of particle size and hydrophilic coating. *Biochem Biophys Res Commun* 1991;177:861-6.
11. Allen TM, Hansen C. Pharmacokinetics of stealth versus conventional liposomes: effect of dose. *Biochim Biophys Acta* 1991;1068:133-41.
12. Yu SE, Chung S, Ha H-S, Kim D-H, Baek S, Kim TY, et al. Nanotheranostics of Pre-Stenotic Vessels By Target Touch-On Signaling of Peptide Navigator. *Advanced Functional Materials* 2022;32:2110368.
13. Swirski FK, Nahrendorf M, Etzrodt M, Wildgruber M, Cortez-Retamozo V, Panizzi P, et al. Identification of splenic reservoir monocytes and their deployment to inflammatory sites. *Science* 2009;325:612-6.
14. Bronte V, Pittet MJ. The spleen in local and systemic regulation of immunity. *Immunity* 2013;39:806-18.

15. Swirski FK, Nahrendorf M. Leukocyte behavior in atherosclerosis, myocardial infarction, and heart failure. *Science* 2013;339:161-6.
16. Kim E, Yang J, Beltran CD, Cho S. Role of spleen-derived monocytes/macrophages in acute ischemic brain injury. *J Cereb Blood Flow Metab* 2014;34:1411-9.
17. Potteaux S, Ait-Oufella H, Mallat Z. Role of splenic monocytes in atherosclerosis. *Curr Opin Lipidol* 2015;26:457-63.
18. Wang NP, Erskine J, Zhang WW, Zheng RH, Zhang LH, Duron G, et al. Recruitment of macrophages from the spleen contributes to myocardial fibrosis and hypertension induced by angiotensin II. *J Renin Angiotensin Aldosterone Syst* 2017;18:1470320317706653.
19. Wang J, Hossain M, Thanabalasuriar A, Gunzer M, Meininger C, Kubes P. Visualizing the function and fate of neutrophils in sterile injury and repair. *Science* 2017;358:111-6.
20. Hou J, Yang X, Li S, Cheng Z, Wang Y, Zhao J, et al. Accessing neuroinflammation sites: Monocyte/neutrophil-mediated drug delivery for cerebral ischemia. *Sci Adv* 2019;5:eaau8301.
21. Krohn-Grimberghe M, Mitchell MJ, Schloss MJ, Khan OF, Courties G, Guimaraes PPG, et al. Nanoparticle-encapsulated siRNAs for gene silencing in the haematopoietic stem-cell niche. *Nat Biomed Eng* 2020;4:1076-89.
22. Senders ML, Meerwaldt AE, van Leent MMT, Sanchez-Gaytan BL, van de Voort JC, Toner YC, et al. Probing myeloid cell dynamics in ischaemic heart disease by nanotracer hot-spot imaging. *Nat Nanotechnol* 2020;15:398-405.
23. Che J, Najer A, Blakney AK, McKay PF, Bellahcene M, Winter CW, et al. Neutrophils Enable Local and Non-Invasive Liposome Delivery to Inflamed Skeletal Muscle and Ischemic Heart. *Adv Mater* 2020;32:e2003598.
24. Kratofil RM, Shim HB, Shim R, Lee WY, Labit E, Sinha S, et al. A monocyte-leptin-angiogenesis pathway critical for repair post-infection. *Nature* 2022;609:166-73.
25. Yu MK, Park J, Jon S. Targeting strategies for multifunctional nanoparticles in cancer imaging and therapy. *Theranostics* 2012;2:3-44.
26. Blanco E, Shen H, Ferrari M. Principles of nanoparticle design for overcoming biological barriers to drug delivery. *Nat Biotechnol* 2015;33:941-51.
27. Asahara T, Murohara T, Sullivan A, Silver M, van der Zee R, Li T, et al. Isolation of putative progenitor endothelial cells for angiogenesis. *Science* 1997;275:964-7.
28. Asahara T, Masuda H, Takahashi T, Kalka C, Pastore C, Silver M, et al. Bone marrow origin of endothelial progenitor cells responsible for postnatal vasculogenesis in physiological and pathological neovascularization. *Circ Res* 1999;85:221-8.
29. Takahashi T, Kalka C, Masuda H, Chen D, Silver M, Kearney M, et al. Ischemia- and cytokine-induced mobilization of bone marrow-derived endothelial progenitor cells for neovascularization. *Nat Med* 1999;5:434-8.

30. Kalka C, Masuda H, Takahashi T, Kalka-Moll WM, Silver M, Kearney M, et al. Transplantation of ex vivo expanded endothelial progenitor cells for therapeutic neovascularization. *Proc Natl Acad Sci U S A* 2000;97:3422-7.
31. Shintani S, Murohara T, Ikeda H, Ueno T, Sasaki K, Duan J, et al. Augmentation of postnatal neovascularization with autologous bone marrow transplantation. *Circulation* 2001;103:897-903.
32. Kamihata H, Matsubara H, Nishiue T, Fujiyama S, Tsutsumi Y, Ozono R, et al. Implantation of bone marrow mononuclear cells into ischemic myocardium enhances collateral perfusion and regional function via side supply of angioblasts, angiogenic ligands, and cytokines. *Circulation* 2001;104:1046-52.
33. Kawamoto A, Gwon HC, Iwaguro H, Yamaguchi JI, Uchida S, Masuda H, et al. Therapeutic potential of ex vivo expanded endothelial progenitor cells for myocardial ischemia. *Circulation* 2001;103:634-7.
34. Kocher AA, Schuster MD, Szabolcs MJ, Takuma S, Burkhoff D, Wang J, et al. Neovascularization of ischemic myocardium by human bone-marrow-derived angioblasts prevents cardiomyocyte apoptosis, reduces remodeling and improves cardiac function. *Nat Med* 2001;7:430-6.
35. Orlic D, Kajstura J, Chimenti S, Jakoniuk I, Anderson SM, Li B, et al. Bone marrow cells regenerate infarcted myocardium. *Nature* 2001;410:701-5.
36. Kamihata H, Matsubara H, Nishiue T, Fujiyama S, Amano K, Iba O, et al. Improvement of collateral perfusion and regional function by implantation of peripheral blood mononuclear cells into ischemic hibernating myocardium. *Arterioscler Thromb Vasc Biol* 2002;22:1804-10.
37. Werner N, Junk S, Laufs U, Link A, Walenta K, Bohm M, et al. Intravenous transfusion of endothelial progenitor cells reduces neointima formation after vascular injury. *Circ Res* 2003;93:e17-24.
38. Kobayashi K, Kondo T, Inoue N, Aoki M, Mizuno M, Komori K, et al. Combination of in vivo angiopoietin-1 gene transfer and autologous bone marrow cell implantation for functional therapeutic angiogenesis. *Arterioscler Thromb Vasc Biol* 2006;26:1465-72.
39. Jeon O, Kang SW, Lim HW, Choi D, Kim DI, Lee SH, et al. Synergistic effect of sustained delivery of basic fibroblast growth factor and bone marrow mononuclear cell transplantation on angiogenesis in mouse ischemic limbs. *Biomaterials* 2006;27:1617-25.
40. Jeon O, Song SJ, Bhang SH, Choi CY, Kim MJ, Kim BS. Additive effect of endothelial progenitor cell mobilization and bone marrow mononuclear cell transplantation on angiogenesis in mouse ischemic limbs. *J Biomed Sci* 2007;14:323-30.
41. Zhang H, Zhang N, Li M, Feng H, Jin W, Zhao H, et al. Therapeutic angiogenesis of bone marrow mononuclear cells (MNCs) and peripheral blood MNCs: transplantation for ischemic hindlimb. *Ann Vasc Surg* 2008;22:238-47.
42. Yang J, Ii M, Kamei N, Alev C, Kwon SM, Kawamoto A, et al. CD34+ cells

- represent highly functional endothelial progenitor cells in murine bone marrow. *PLoS One* 2011;6:e20219.
43. Brenes RA, Jadlowiec CC, Bear M, Hashim P, Protack CD, Li X, et al. Toward a mouse model of hind limb ischemia to test therapeutic angiogenesis. *J Vasc Surg* 2012;56:1669-79; discussion 79.
  44. Yao Z, Liu H, Yang M, Bai Y, Zhang B, Wang C, et al. Bone marrow mesenchymal stem cell-derived endothelial cells increase capillary density and accelerate angiogenesis in mouse hindlimb ischemia model. *Stem Cell Res Ther* 2020;11:221.
  45. Yamada H, Sakata N, Nishimura M, Tanaka T, Shimizu M, Yoshimatsu G, et al. Xenotransplantation of neonatal porcine bone marrow-derived mesenchymal stem cells improves murine hind limb ischemia through lymphangiogenesis and angiogenesis. *Xenotransplantation* 2021;28:e12693.
  46. Beaudry P, Hida Y, Udagawa T, Alwayn IP, Greene AK, Arsenault D, et al. Endothelial progenitor cells contribute to accelerated liver regeneration. *J Pediatr Surg* 2007;42:1190-8.
  47. Nakamura T, Torimura T, Sakamoto M, Hashimoto O, Taniguchi E, Inoue K, et al. Significance and therapeutic potential of endothelial progenitor cell transplantation in a cirrhotic liver rat model. *Gastroenterology* 2007;133:91-107.e1.
  48. Nakamura T, Torimura T, Iwamoto H, Masuda H, Naitou M, Koga H, et al. Prevention of liver fibrosis and liver reconstitution of DMN-treated rat liver by transplanted EPCs. *Eur J Clin Invest* 2012;42:717-28.
  49. Uda Y, Hirano T, Son G, Iimuro Y, Uyama N, Yamanaka J, et al. Angiogenesis is crucial for liver regeneration after partial hepatectomy. *Surgery* 2013;153:70-7.
  50. Lin CK, Huang TH, Yang CT, Shi CS. Roles of lung-recruited monocytes and pulmonary Vascular Endothelial Growth Factor (VEGF) in resolving Ventilator-Induced Lung Injury (VILI). *PLoS One* 2021;16:e0248959.
  51. Song Y, Wang Z, Liu L, Wang D, Zhang J. The level of circulating endothelial progenitor cells may be associated with the occurrence and recurrence of chronic subdural hematoma. *Clinics (Sao Paulo)* 2013;68:1084-8.
  52. Martínez-Muriana A, Pastor D, Mancuso R, Rando A, Osta R, Martínez S, et al. Combined intramuscular and intraspinal transplant of bone marrow cells improves neuromuscular function in the SOD1(G93A) mice. *Stem Cell Res Ther* 2020;11:53.
  53. Drixler TA, Vogten MJ, Ritchie ED, van Vroonhoven TJ, Gebbink MF, Voest EE, et al. Liver regeneration is an angiogenesis- associated phenomenon. *Ann Surg* 2002;236:703-11; discussion 11-2.
  54. Wollert KC, Meyer GP, Lotz J, Ringes-Lichtenberg S, Lippolt P, Breidenbach C, et al. Intracoronary autologous bone-marrow cell transfer after myocardial infarction: the BOOST randomised controlled clinical trial. *Lancet* 2004;364:141-8.
  55. Schächinger V, Erbs S, Elsässer A, Haberbosch W, Hambrecht R, Hölschermann H, et al. Intracoronary bone marrow-derived progenitor cells in acute myocardial infarction. *N Engl J Med* 2006;355:1210-21.

56. Tendera M, Wojakowski W, Rużyło W, Chojnowska L, Kepka C, Tracz W, et al. Intracoronary infusion of bone marrow-derived selected CD34+CXCR4+ cells and non-selected mononuclear cells in patients with acute STEMI and reduced left ventricular ejection fraction: results of randomized, multicentre Myocardial Regeneration by Intracoronary Infusion of Selected Population of Stem Cells in Acute Myocardial Infarction (REGENT) Trial. *Eur Heart J* 2009;30:1313-21.
57. Quyyumi AA, Waller EK, Murrow J, Esteves F, Galt J, Oshinski J, et al. CD34(+) cell infusion after ST elevation myocardial infarction is associated with improved perfusion and is dose dependent. *Am Heart J* 2011;161:98-105.
58. Povsic TJ, Junge C, Nada A, Schatz RA, Harrington RA, Davidson CJ, et al. A phase 3, randomized, double-blinded, active-controlled, unblinded standard of care study assessing the efficacy and safety of intramyocardial autologous CD34+ cell administration in patients with refractory angina: design of the RENEW study. *Am Heart J* 2013;165:854-61.e2.
59. Quyyumi AA, Vasquez A, Kereiakes DJ, Klapholz M, Schaer GL, Abdel-Latif A, et al. PreSERVE-AMI: A Randomized, Double-Blind, Placebo-Controlled Clinical Trial of Intracoronary Administration of Autologous CD34+ Cells in Patients With Left Ventricular Dysfunction Post STEMI. *Circ Res* 2017;120:324-31.
60. Wollert KC, Meyer GP, Müller-Ehmsen J, Tschöpe C, Bonatjee V, Larsen AI, et al. Intracoronary autologous bone marrow cell transfer after myocardial infarction: the BOOST-2 randomised placebo-controlled clinical trial. *Eur Heart J* 2017;38:2936-43.
61. Kawamoto A, Katayama M, Handa N, Kinoshita M, Takano H, Horii M, et al. Intramuscular transplantation of G-CSF-mobilized CD34(+) cells in patients with critical limb ischemia: a phase I/IIa, multicenter, single-blinded, dose-escalation clinical trial. *Stem Cells* 2009;27:2857-64.
62. Kinoshita M, Fujita Y, Katayama M, Baba R, Shibakawa M, Yoshikawa K, et al. Long-term clinical outcome after intramuscular transplantation of granulocyte colony stimulating factor-mobilized CD34 positive cells in patients with critical limb ischemia. *Atherosclerosis* 2012;224:440-5.
63. Losordo DW, Kibbe MR, Mendelsohn F, Marston W, Driver VR, Sharafuddin M, et al. A randomized, controlled pilot study of autologous CD34+ cell therapy for critical limb ischemia. *Circ Cardiovasc Interv* 2012;5:821-30.
64. Fujita Y, Kinoshita M, Furukawa Y, Nagano T, Hashimoto H, Hiram Y, et al. Phase II clinical trial of CD34+ cell therapy to explore endpoint selection and timing in patients with critical limb ischemia. *Circ J* 2014;78:490-501.
65. Hoover-Plow J, Gong Y. Challenges for heart disease stem cell therapy. *Vasc Health Risk Manag* 2012;8:99-113.
66. Hou L, Kim JJ, Woo YJ, Huang NF. Stem cell-based therapies to promote angiogenesis in ischemic cardiovascular disease. *Am J Physiol Heart Circ Physiol* 2016;310:H455-65.
67. Fujita Y, Kawamoto A. Stem cell-based peripheral vascular regeneration. *Adv*

- Drug Deliv Rev 2017;120:25-40.
68. Keighron C, Lyons CJ, Creane M, O'Brien T, Liew A. Recent Advances in Endothelial Progenitor Cells Toward Their Use in Clinical Translation. *Front Med (Lausanne)* 2018;5:354.
  69. Bianconi V, Sahebkar A, Kovanen P, Bagaglia F, Ricciuti B, Calabrò P, et al. Endothelial and cardiac progenitor cells for cardiovascular repair: A controversial paradigm in cell therapy. *Pharmacol Ther* 2018;181:156-68.
  70. Fisher SA, Zhang H, Doree C, Mathur A, Martin-Rendon E. Stem cell treatment for acute myocardial infarction. *Cochrane Database Syst Rev* 2015;2015:Cd006536.
  71. Kang J, Kim TW, Hur J, Kim HS. Strategy to Prime the Host and Cells to Augment Therapeutic Efficacy of Progenitor Cells for Patients with Myocardial Infarction. *Front Cardiovasc Med* 2016;3:46.
  72. Hoenig MR, Bianchi C, Sellke FW. Hypoxia inducible factor-1 alpha, endothelial progenitor cells, monocytes, cardiovascular risk, wound healing, cobalt and hydralazine: a unifying hypothesis. *Curr Drug Targets* 2008;9:422-35.
  73. Lee SW, Jeong HK, Lee JY, Yang J, Lee EJ, Kim SY, et al. Hypoxic priming of mESCs accelerates vascular-lineage differentiation through HIF1-mediated inverse regulation of Oct4 and VEGF. *EMBO Mol Med* 2012;4:924-38.
  74. Zhang J, Liu Q, Fang Z, Hu X, Huang F, Tang L, et al. Hypoxia induces the proliferation of endothelial progenitor cells via upregulation of Apelin/APLNR/MAPK signaling. *Mol Med Rep* 2016;13:1801-6.
  75. Pugh CW, Ratcliffe PJ. Regulation of angiogenesis by hypoxia: role of the HIF system. *Nat Med* 2003;9:677-84.
  76. Weidemann A, Johnson RS. Biology of HIF-1alpha. *Cell Death Differ* 2008;15:621-7.
  77. Tsai CC, Chen YJ, Yew TL, Chen LL, Wang JY, Chiu CH, et al. Hypoxia inhibits senescence and maintains mesenchymal stem cell properties through down-regulation of E2A-p21 by HIF-TWIST. *Blood* 2011;117:459-69.
  78. Creager MA, Olin JW, Belch JJ, Moneta GL, Henry TD, Rajagopalan S, et al. Effect of hypoxia-inducible factor-1alpha gene therapy on walking performance in patients with intermittent claudication. *Circulation* 2011;124:1765-73.
  79. Kütscher C, Lampert FM, Kunze M, Markfeld-Erol F, Stark GB, Finkenzeller G. Overexpression of hypoxia-inducible factor-1 alpha improves vasculogenesis-related functions of endothelial progenitor cells. *Microvasc Res* 2016;105:85-92.
  80. Choo SY, Yoon SH, Lee DJ, Lee SH, Li K, Koo IH, et al. Runx3 inhibits endothelial progenitor cell differentiation and function via suppression of HIF-1 $\alpha$  activity. *Int J Oncol* 2019;54:1327-36.
  81. Han Y, Gong T, Zhang C, Dissanayaka WL. HIF-1 $\alpha$  Stabilization Enhances Angio-/Vasculogenic Properties of SHED. *J Dent Res* 2020;99:804-12.
  82. Cipolleschi MG, Dello Sbarba P, Olivotto M. The role of hypoxia in the maintenance of hematopoietic stem cells. *Blood* 1993;82:2031-7.

83. Nombela-Arrieta C, Pivarnik G, Winkel B, Canty KJ, Harley B, Mahoney JE, et al. Quantitative imaging of haematopoietic stem and progenitor cell localization and hypoxic status in the bone marrow microenvironment. *Nat Cell Biol* 2013;15:533-43.
84. Wang LD, Wagers AJ. Dynamic niches in the origination and differentiation of haematopoietic stem cells. *Nat Rev Mol Cell Biol* 2011;12:643-55.
85. Morrison SJ, Scadden DT. The bone marrow niche for haematopoietic stem cells. *Nature* 2014;505:327-34.
86. Liu C, Tsai AL, Li PC, Huang CW, Wu CC. Endothelial differentiation of bone marrow mesenchyme stem cells applicable to hypoxia and increased migration through Akt and NF $\kappa$ B signals. *Stem Cell Res Ther* 2017;8:29.
87. Lin Y, Liu B, Deng T, Zhong J, Feng Z, Zeng Q, et al. Normoxia is not favorable for maintaining stemness of human endothelial progenitor cells. *Stem Cell Res* 2019;38:101464.
88. Maxwell PH, Wiesener MS, Chang GW, Clifford SC, Vaux EC, Cockman ME, et al. The tumour suppressor protein VHL targets hypoxia-inducible factors for oxygen-dependent proteolysis. *Nature* 1999;399:271-5.
89. Epstein AC, Gleadle JM, McNeill LA, Hewitson KS, O'Rourke J, Mole DR, et al. *C. elegans* EGL-9 and mammalian homologs define a family of dioxygenases that regulate HIF by prolyl hydroxylation. *Cell* 2001;107:43-54.
90. Fong GH, Takeda K. Role and regulation of prolyl hydroxylase domain proteins. *Cell Death Differ* 2008;15:635-41.
91. Mueller S, Millonig G, Waite GN. The GOX/CAT system: a novel enzymatic method to independently control hydrogen peroxide and hypoxia in cell culture. *Adv Med Sci* 2009;54:121-35.
92. Simonsen LO, Harbak H, Bennekou P. Cobalt metabolism and toxicology--a brief update. *Sci Total Environ* 2012;432:210-5.
93. Yang M, Su H, Soga T, Kranc KR, Pollard PJ. Prolyl hydroxylase domain enzymes: important regulators of cancer metabolism. *Hypoxia (Auckl)* 2014;2:127-42.
94. Rana NK, Singh P, Koch B. CoCl<sub>2</sub> simulated hypoxia induce cell proliferation and alter the expression pattern of hypoxia associated genes involved in angiogenesis and apoptosis. *Biol Res* 2019;52:12.
95. Zhang Y, Zhao HJ, Xia XR, Diao FY, Ma X, Wang J, et al. Hypoxia-induced and HIF1 $\alpha$ -VEGF-mediated tight junction dysfunction in choriocarcinoma cells: Implications for preeclampsia. *Clin Chim Acta* 2019;489:203-11.
96. Lazzara F, Trotta MC, Platania CBM, D'Amico M, Petrillo F, Galdiero M, et al. Stabilization of HIF-1 $\alpha$  in Human Retinal Endothelial Cells Modulates Expression of miRNAs and Proangiogenic Growth Factors. *Front Pharmacol* 2020;11:1063.
97. Rinderknecht H, Ehnert S, Braun B, Histing T, Nussler AK, Linnemann C. The Art of Inducing Hypoxia. *Oxygen* 2021;1:46-61.
98. Mitchell C, Willenbring H. A reproducible and well-tolerated method for 2/3 partial hepatectomy in mice. *Nat Protoc* 2008;3:1167-70.

99. Larese Filon F, Crosera M, Timeus E, Adami G, Bovenzi M, Ponti J, et al. Human skin penetration of cobalt nanoparticles through intact and damaged skin. *Toxicol In Vitro* 2013;27:121-7.
100. Wang Z, Chen Z, Zuo Q, Song F, Wu D, Cheng W, et al. Reproductive toxicity in adult male rats following intra-articular injection of cobalt-chromium nanoparticles. *J Orthop Sci* 2013;18:1020-6.
101. Zheng F, Luo Z, Zheng C, Li J, Zeng J, Yang H, et al. Comparison of the neurotoxicity associated with cobalt nanoparticles and cobalt chloride in Wistar rats. *Toxicol Appl Pharmacol* 2019;369:90-9.

## ABSTRACT(IN KOREAN)

비장의 나노-저산소화를 통한 생체 내 리프로그래밍을 바탕으로  
혈관 형성 세포 활용 치료 전략 수립

&lt;지도교수 성학준&gt;

연세대학교 대학원 의학과

정 세 용

타겟팅 나노 입자가 타겟 부위에 도달하는 용량이 전체 주입 용량의 0.7%에 불과하다는 메타분석 결과가 있는데, 그 주요 원인 중 하나는 비장이 혈액의 필터로서 나노 입자를 걸러내기 때문이다. 그러나 만약 비장에서 걸러진 나노 입자가 비장 세포와 함께 타겟 부위로 이동을 한다면 비장이 꼭 타겟팅의 장애물이 될 필요는 없는데, 실제로 비장의 단핵세포는 혈관 허혈 부위로 이동한다는 것이 알려져 있다. 이러한 내용은 혈관 형성 세포 치료에 활용해 볼 수 있는데, 이 치료 방법으로 수십여 번의 임상 실험이 진행되었으나 용량과 전달 방법에서 한계점을 극복하지 못하고 있다. 본 연구에서는 비장 단핵세포를 생체 내에서 혈관 형성 세포로 리프로그래밍을 시도하였으며, 그 수단으로써 나노-저산소화를 이용하였다. 저산소 환경 모사체를 담지한 나노 입자는 불가피하게 비장 단핵세포에 의해 걸러졌고, 비장 단핵세포는 혈관 형성 세포가 되어 혈관 형성을 촉진하였다. 또한 이렇게 확보된 혈관 형성 세포는 기존 치료 용량의 20배가 넘었으며, 이들은 자연적으로 혈관 허혈 부위로 이동하는 양상을 보여줌으로써, 기존의 혈관 형성 세포 치료의 용량 및 전달 방법 문제를 효과적으로 해결할 수 있었다. 이에 따라, 이 전략은 마우스 하지 허혈 모델에서 기존 치료 방법 보다 효과적인 혈관 재생과 혈류 회복을 보여줬다. 나아가, 마우스 간 70% 절제 모델에서도 효과적인 혈관 재생 및 간 조직 재생 효과를 보여주었다. 결론적으로, 비장의 나노-저산소화를 통한 생체 내 리프로그래밍 전략은 기존 혈관 형성 세포 치료의 용량과 전달 방법 문제를 효과적으로 해결하는 치료

전략이 될 수 있을 것이다.

---

핵심되는 말 : 타겟팅 나노 입자, 비장, 염증 부위, 혈관 형성 세포, 혈관 재생

## PUBLICATION LIST

1. Chung S, Kim SY, Lee K, Baek S, Ha H-S, Kim D-H, et al. In Situ Reprogrammings of Splenic CD11b<sup>+</sup> Cells by Nano-Hypoxia to Promote Inflamed Damage Site-Specific Angiogenesis. *Advanced Functional Materials* 2023;33:2302817.